

European Research Council
Established by the European Commission



Equation of state constraints from binary neutron star mergers

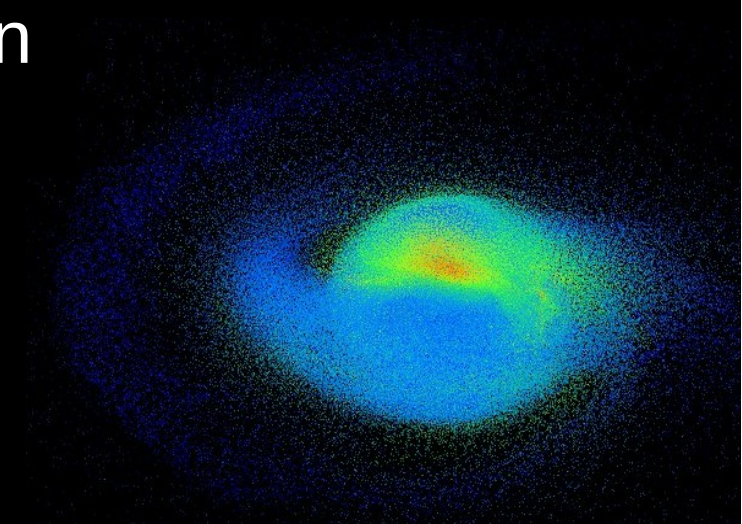
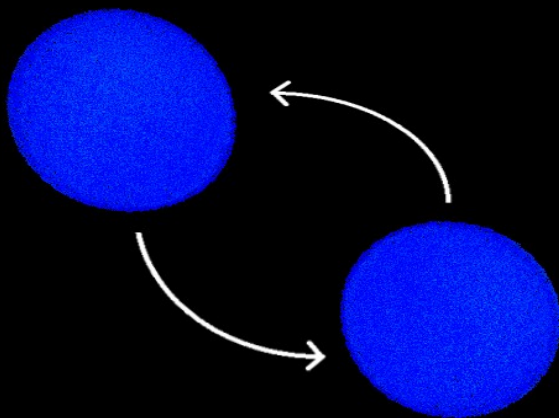
3rd HEL.A.S Summer School and DAAD School

Neutron stars and gravitational waves

Frappe city, 8-12/10/2018

Andreas Bauswein

(GSI Darmstadt)



FAIR next generation scientists - 6th Edition Workshop

20-24 May 2019
Grand Hotel Arenzano, Genova, Italy
Europe/Berlin timezone

Workshop for young scientists with research interests focused on physics at FAIR

Overview and Scientific
Programme

Registration and Abstract
Submission

[Complete the Form](#)

Conference Fee

Accommodation

Venue and Travel Info

Support

fairness@fias.uni-fran...

FAIRness 2019 is the sixth edition in series of workshops designed to bring together excellent international young scientists with research interests focused on physics at FAIR.

The topics of the workshop cover a wide range of aspects in both theoretical developments and current experimental status, concentrated around the four scientific pillars of FAIR. There will be an inspiring mixture of new theoretical developments and experimental research:

- Atomic and plasma physics, biophysics, material sciences and applications
- Nuclear structure, astrophysics and reactions
- Physics of hot and dense nuclear matter, QCD phase transitions and critical point
- Hadron Spectroscopy, Hadron Structure, Hadrons in matter and Hypernuclei
- Experimental programs APPA, CBM, HADES, NUSTAR, PANDA, as well as BES, NICA and the RHIC beam energy scan



Registration and Abstract Submission Deadline: 1 January 2019

Organizers: Andreas Bauswein, Marco Destefanis, Tetyana Galatyuk (chair), Claudia Ratti and Laura Tolos

- ▶ <https://indico.gsi.de/event/7684/overview>
- ▶ Deadline: 1 January 2019



Scientific aspects of NS mergers

- ▶ NS mergers likely progenitors of short gamma-ray bursts (observed since the 70ies)
- ▶ NS mergers as sources of heavy elements forged by the rapid neutron-capture process
- ▶ Electromagnetic transient powered by nuclear decays during/after r-process (“kilonova”, “macronova”, ...)
 - UV, optical, IR → targets for triggered or blind searches (time-domain astronomy)
- ▶ Various other types of em counterparts
- ▶ Strong emitters of GWs
 - population properties: rates, masses, ... → stellar astrophysics
 - EoS of nuclear matter / stellar properties of NSs
 - (NS mergers probe cold and hot matter – pre- and post-merger)
- ▶ ...

Outline

Focus of this talk on EoS impact / constraints

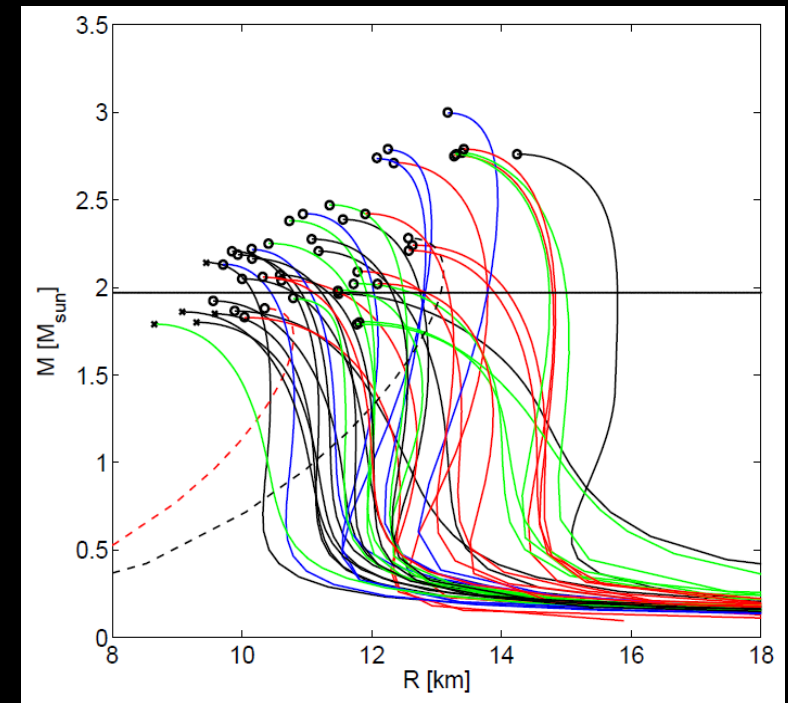
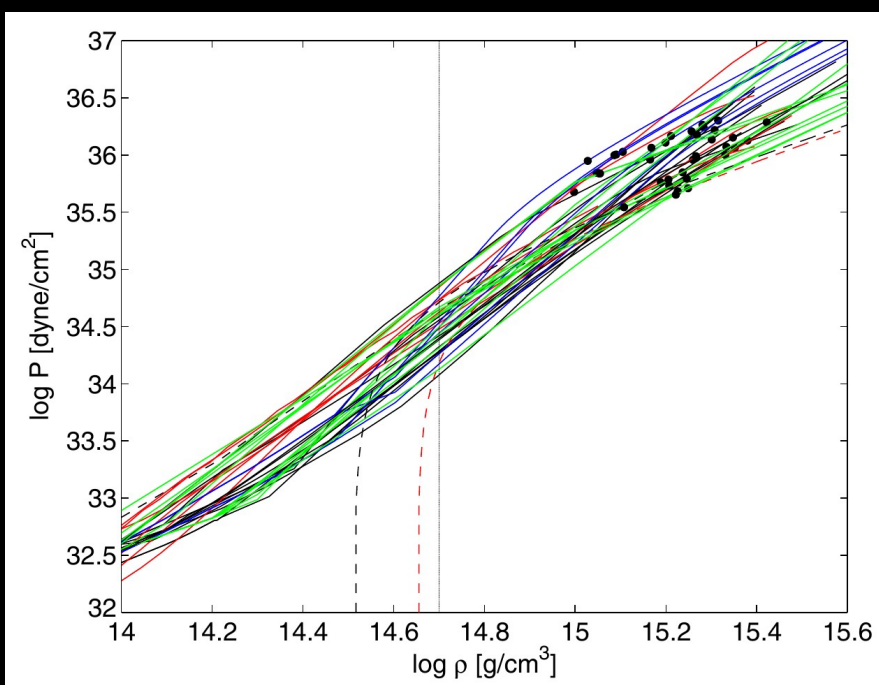
- ▶ Overview / introduction
 - ▶ Ejecta properties and simulations
 - ▶ Tidal deformability
 - ▶ Collapse behavior
 - ▶ NS radius constraints from GW170817
 - ▶ dominant postmerger GW emission
 - NS radius measurements
 - maximum mass and other EoS constraints
 - ▶ Signatures of the QCD phase transition
- 
- presence
- future

Importance of high-density EoS

- ▶ Understand properties of high-density matter (hardly accessible by laboratory experiments – theoretically challenging)
 - e.g. nuclear parameter/models (also important for nucleosynthesis models)
 - phase transition to hyperonic matter? Quark matter?
- ▶ Stellar properties of NS (observationally challenging)
 - EoS affects dynamics/phenomenology of mergers (e.g em counterparts, nucleosynthesis, GRBs), supernovae, NS cooling,

Holy grail: EoS and R(M)

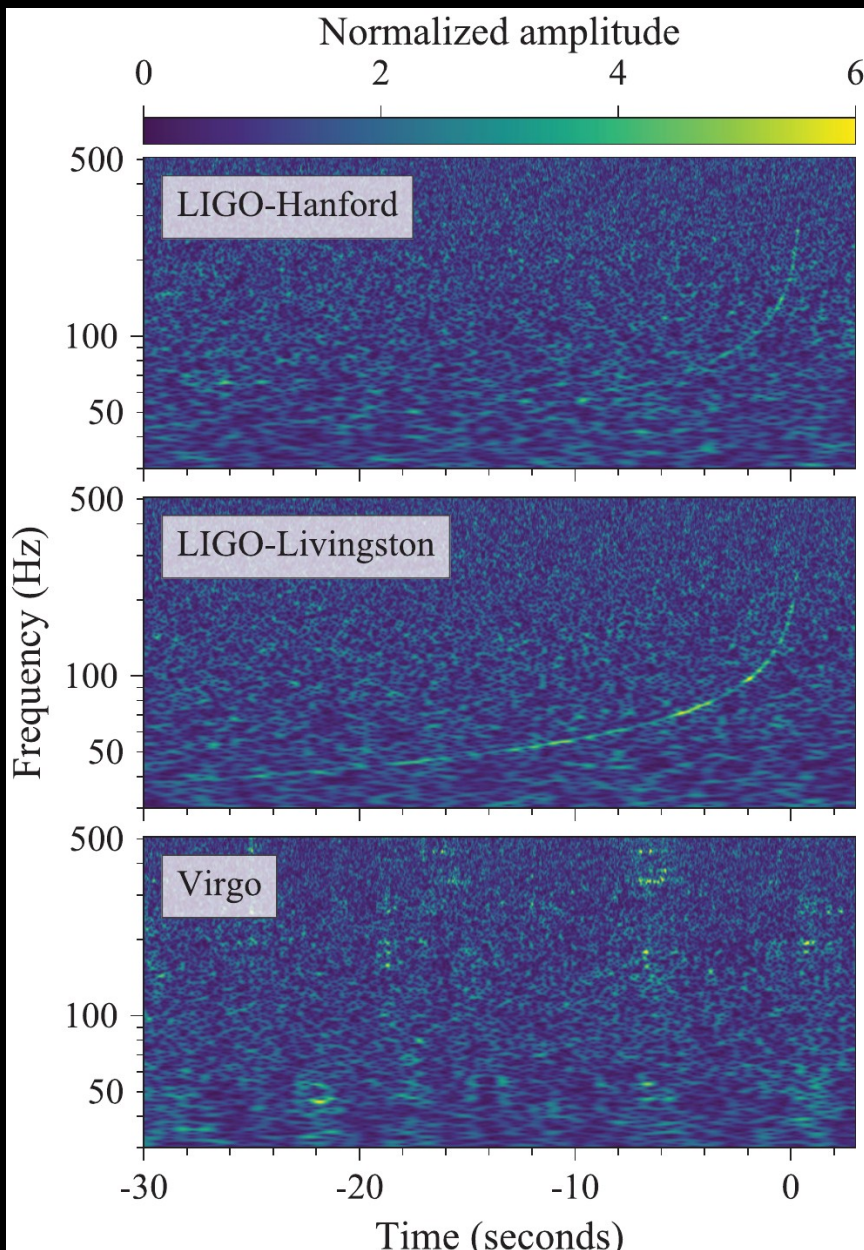
- Mass-radius relation (of non-rotating NSs) and EoS are uniquely linked through Tolman-Oppenheimer-Volkoff (TOV) equations



Theory: $P(\rho)$ currently Observation: $R(M)$
 ← → future

- NS properties (of non-rotating stars) and EoS properties are equivalent !!!
- NS radii are the critical quantity to learn about EoS (generally tough to measure)
(not all displayed EoS compatible with all current constraints)

GW170817

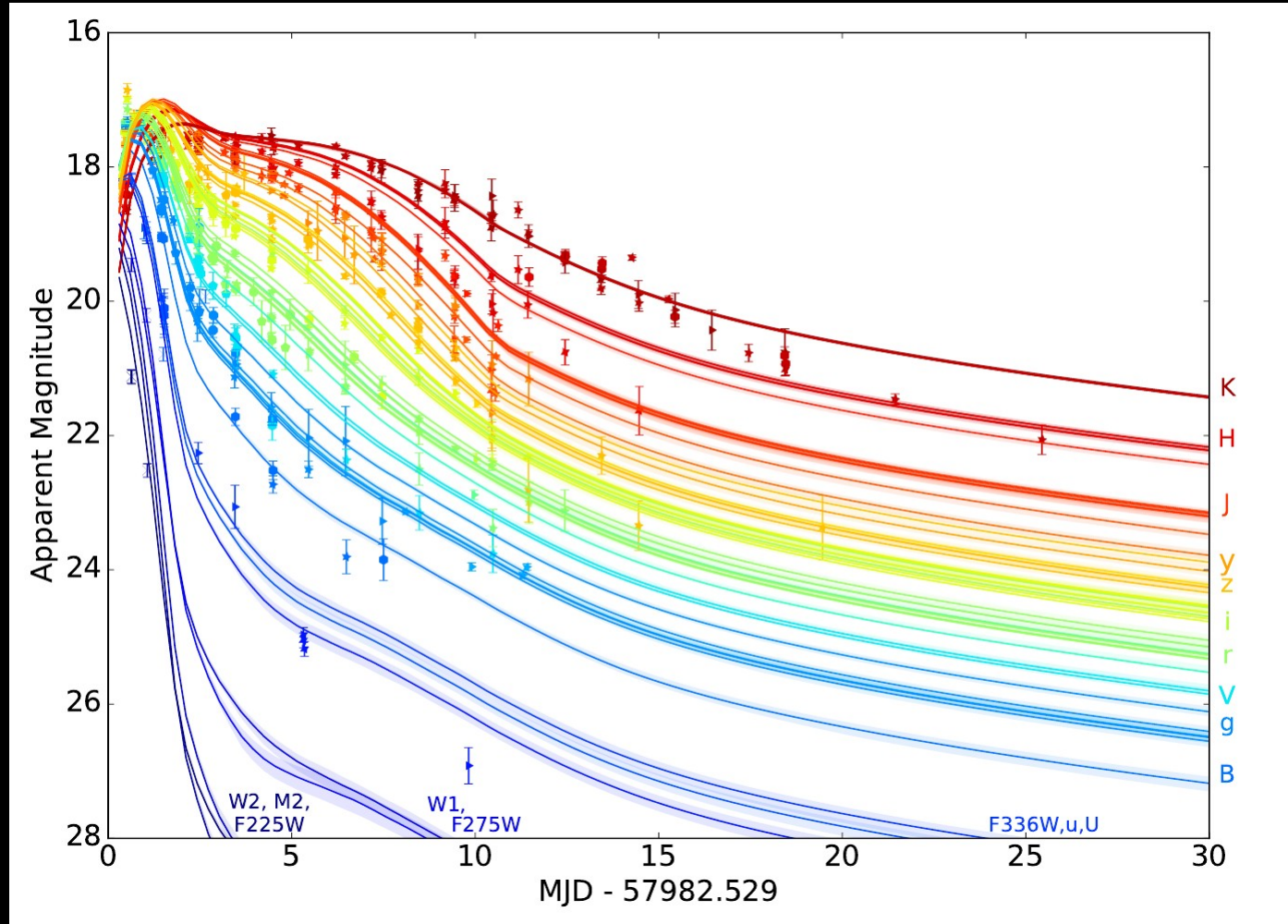


	Low-spin priors ($ \chi \leq 0.05$)
Primary mass m_1	$1.36\text{--}1.60 M_{\odot}$
Secondary mass m_2	$1.17\text{--}1.36 M_{\odot}$
Chirp mass \mathcal{M}	$1.188^{+0.004}_{-0.002} M_{\odot}$
Mass ratio m_2/m_1	$0.7\text{--}1.0$
Total mass m_{tot}	$2.74^{+0.04}_{-0.01} M_{\odot}$
Radiated energy E_{rad}	$> 0.025 M_{\odot} c^2$
Luminosity distance D_L	$40^{+8}_{-14} \text{ Mpc}$
Viewing angle Θ	$\leq 55^\circ$
Using NGC 4993 location	$\leq 28^\circ$
Combined dimensionless tidal deformability $\tilde{\Lambda}$	≤ 800
Dimensionless tidal deformability $\Lambda(1.4M_{\odot})$	≤ 800

Chirp-like signal → compact binary merger
 Shape reveals masses → only compatible with NSs
 → constraints on tidal deformability
 → triggered some follow-up observations

See Chatzioannou's talk

Observations UVOIR – combined from different groups/observations



- ▶ From early blue to red
- ▶ Reasonable agreement with theoretical expectations

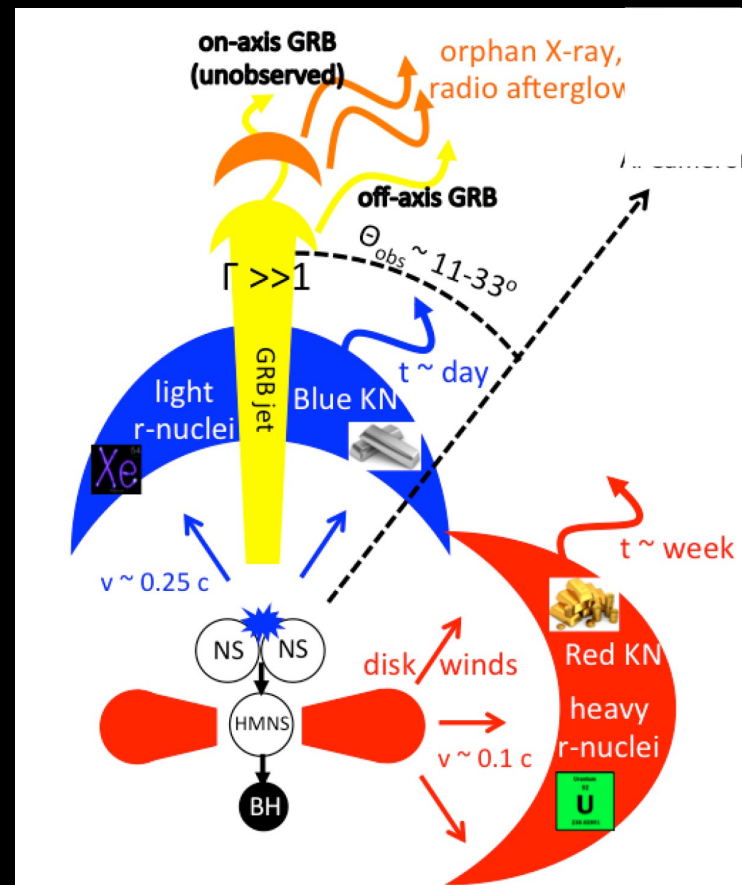
Villar et al. 2018

Observations

- ▶ Many IR/opt/UV observations by many groups
- ▶ Different interpretations / modeling
- ▶ Red and blue component
- ▶ Spectral features?
- ▶ Derived total ejecta masses all in the range 0.03 ... 0.05 Msun

Chronock et al. 2017, Levan & Tanvir 2017,
 Kasliwal et al. 2017, Coulter et al. 2017, Allam
 et al. 2017, Yang et al. 2017, Arcavi et al.
 2017, Kilpatrick et al. 2017, McCully et al.
 2017, Pian et al. 2017, Arcavi et al. 2017,
 Evans et al. 2017, Drout et al. 2017 Lipunov
 et al. 2017, Cowperthwaite et al. 2017, Smartt
 et al. 2017, Shappee et al. 2017, Nicholl et al.
 2017, Kasen et al. 2017, Tanaka et al. 2017,

Reference	$m_{\text{dyn}} [M_{\odot}]$	$m_w [M_{\odot}]$
Abbott et al. (2017a)	0.001 – 0.01	–
Arcavi et al. (2017)	–	0.02 – 0.025
Cowperthwaite et al. (2017)	0.04	0.01
Chornock et al. (2017)	0.035	0.02
Evans et al. (2017)	0.002 – 0.03	0.03 – 0.1
Kasen et al. (2017)	0.04	0.025
Kasliwal et al. (2017b)	> 0.02	> 0.03
Nicholl et al. (2017)	0.03	–
Perego et al. (2017)	0.005 – 0.01	$10^{-5} – 0.024$
Rosswog et al. (2017)	0.01	0.03
Smartt et al. (2017)	0.03 – 0.05	0.018
Tanaka et al. (2017a)	0.01	0.03
Tanvir et al. (2017)	0.002 – 0.01	0.015
Troja et al. (2017)	0.001 – 0.01	0.015 – 0.03

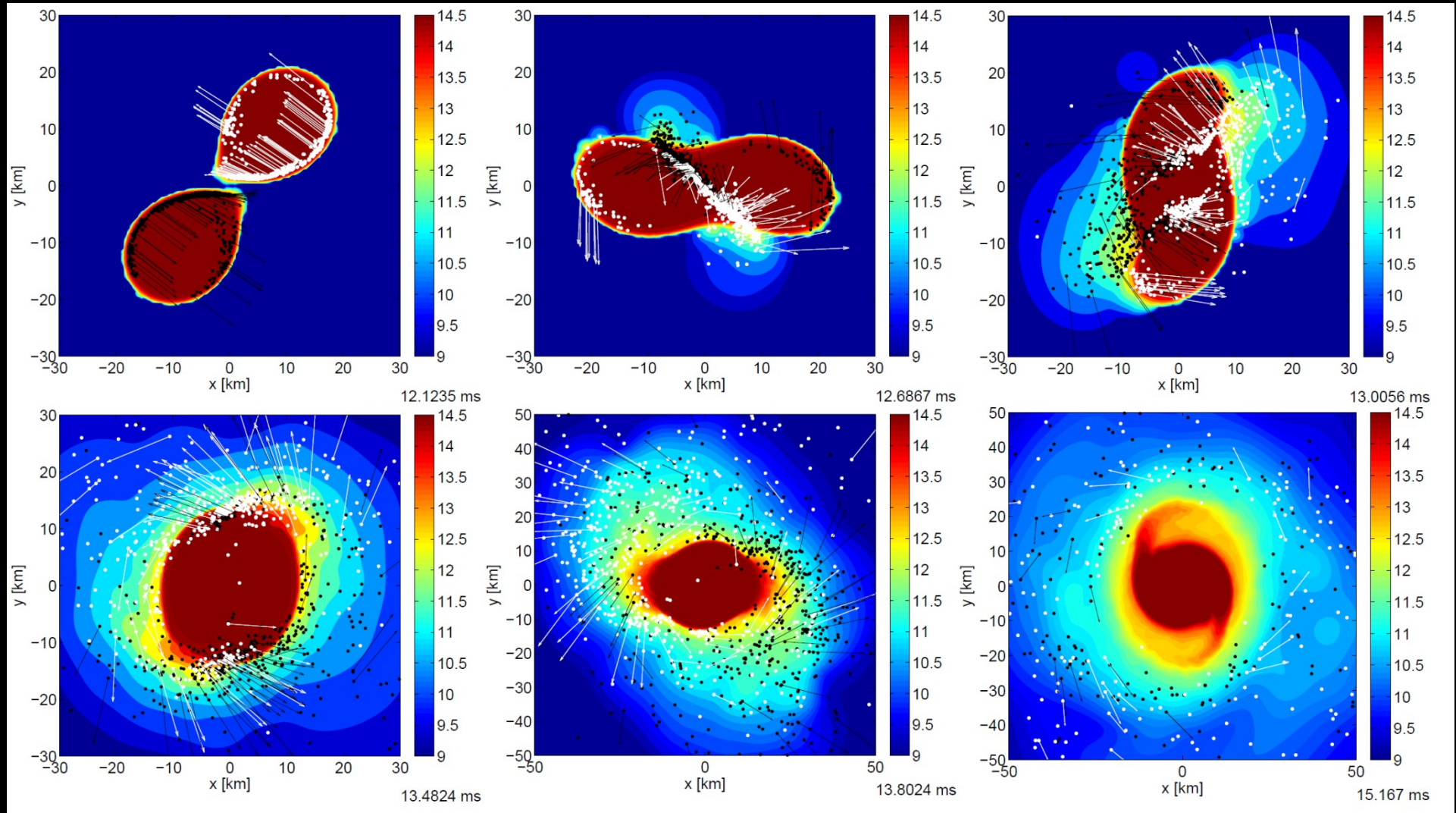


Simulation results – ejecta

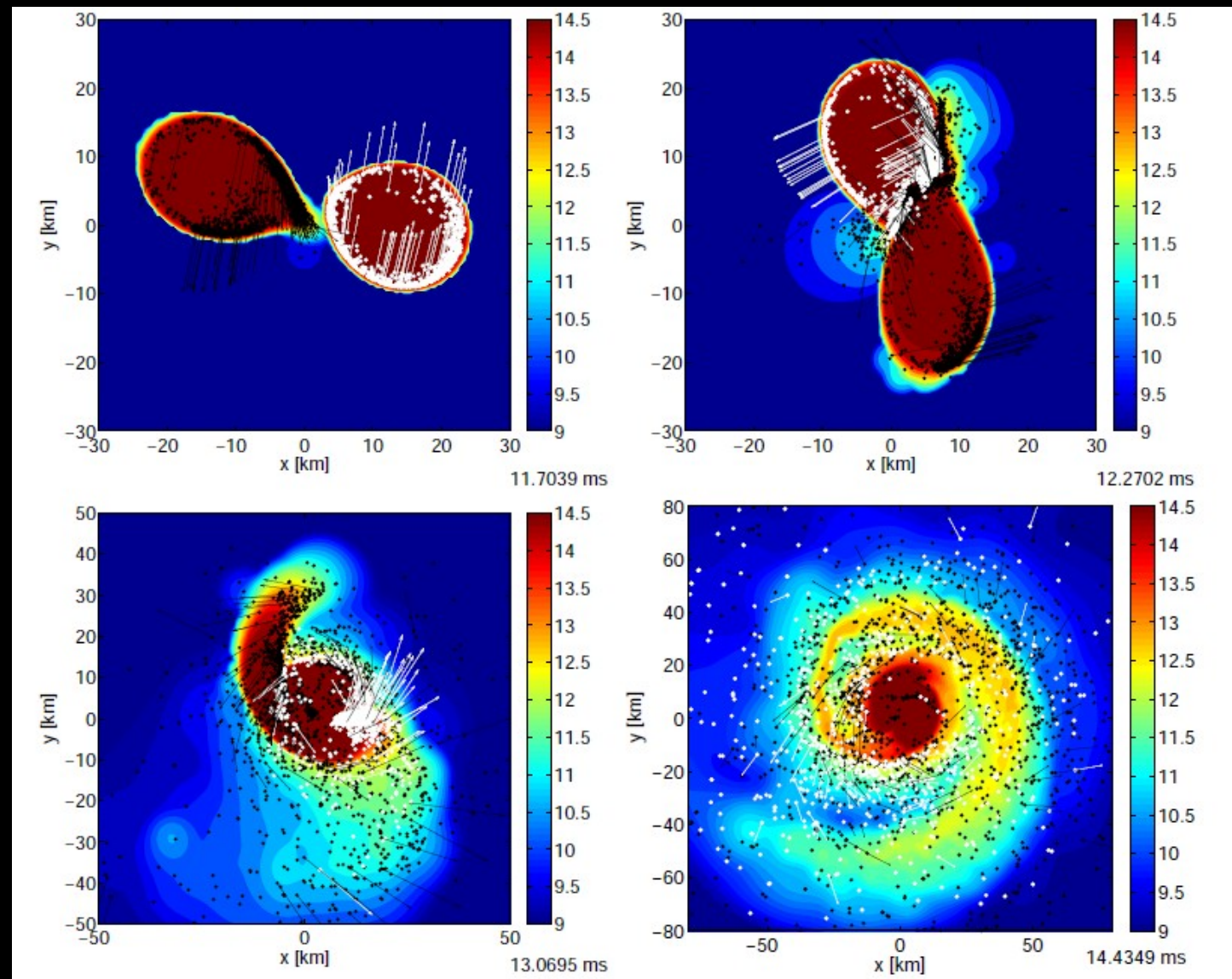
(EoS and binary mass dependence)

Simulations

Dots trace ejecta (DD2 EoS 1.35-1.35 M_{sun})



Asymmetric mergers

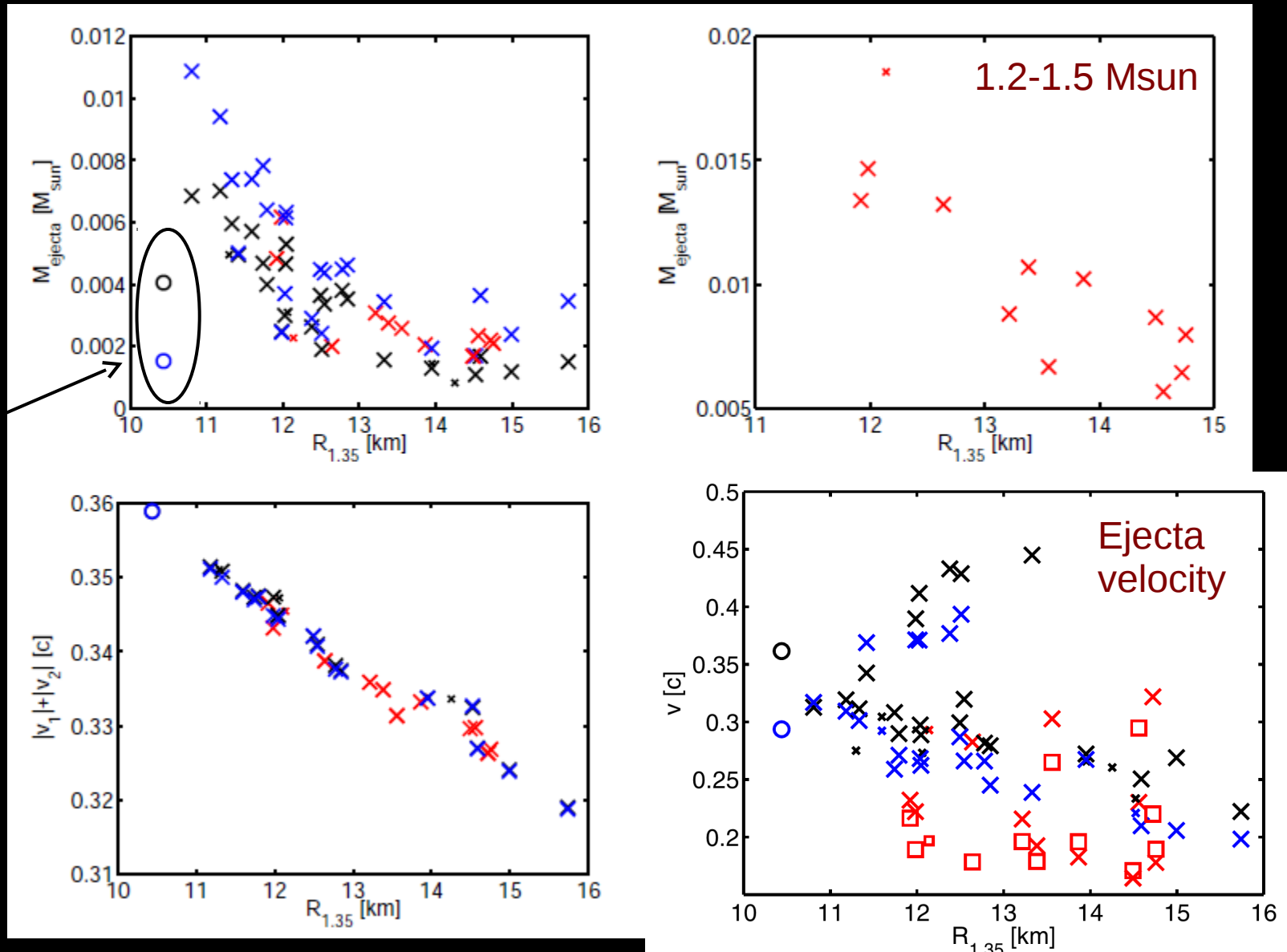


→ larger tidal component, larger total ejecta masses

Bauswein et al. 2013

Ejecta mass dependence

Prompt collapse

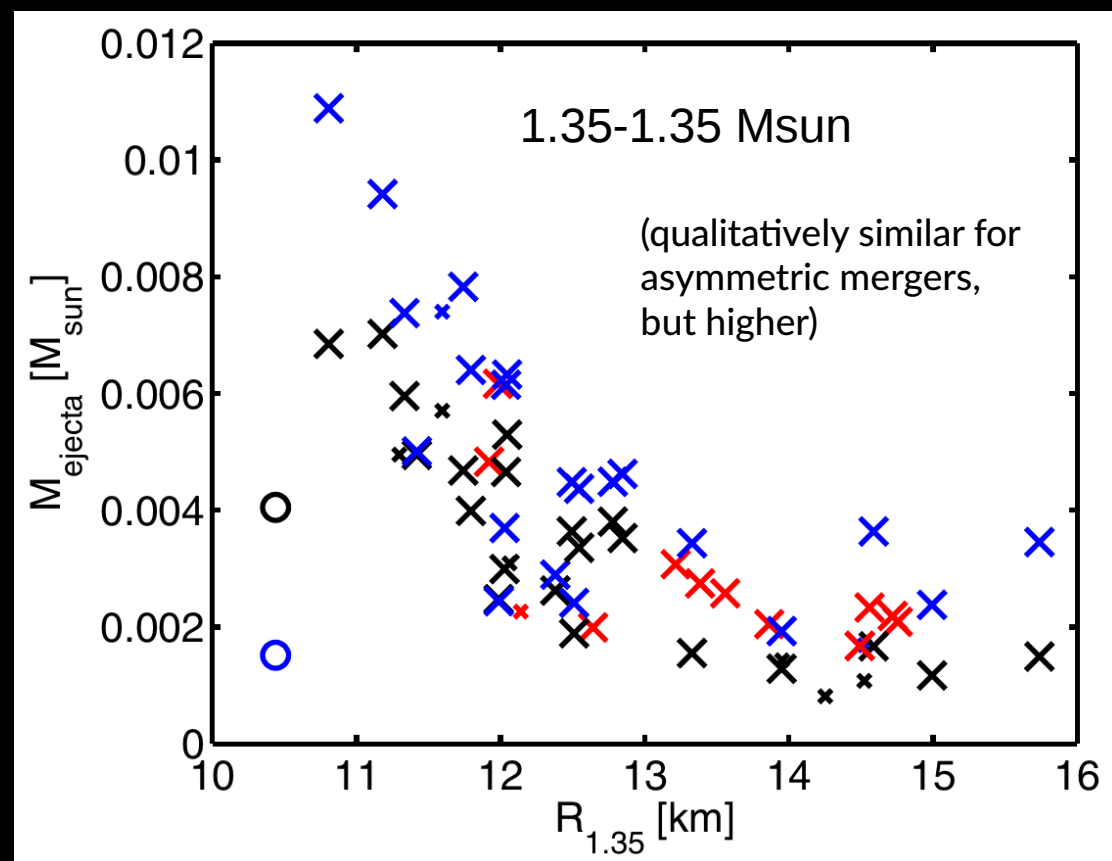


Different EoSs characterized by radii of 1.35 M_{\odot} NSs (note importance of thermal effects)

Coarse picture: EoS dependence of ejecta mass

- ▶ Ejecta mass 0.03-0.05 Msun in GW170817
- ▶ Excludes tentatively very stiff EoSs
- ▶ Excludes tentatively very soft EoSs – prompt collapse !!!
- ▶ Warning: very hard to be quantitative

Reference	$m_{\text{dyn}} [M_{\odot}]$	$m_w [M_{\odot}]$
Abbott et al. (2017a)	0.001 – 0.01	–
Arcavi et al. (2017)	–	0.02 – 0.025
Cowperthwaite et al. (2017)	0.04	0.01
Chornock et al. (2017)	0.035	0.02
Evans et al. (2017)	0.002 – 0.03	0.03 – 0.1
Kasen et al. (2017)	0.04	0.025
Kasliwal et al. (2017b)	> 0.02	> 0.03
Nicholl et al. (2017)	0.03	–
Perego et al. (2017)	0.005 – 0.01	$10^{-5} – 0.024$
Rosswog et al. (2017)	0.01	0.03
Smartt et al. (2017)	0.03 – 0.05	0.018
Tanaka et al. (2017a)	0.01	0.03
Tanvir et al. (2017)	0.002 – 0.01	0.015
Troja et al. (2017)	0.001 – 0.01	0.015 – 0.03

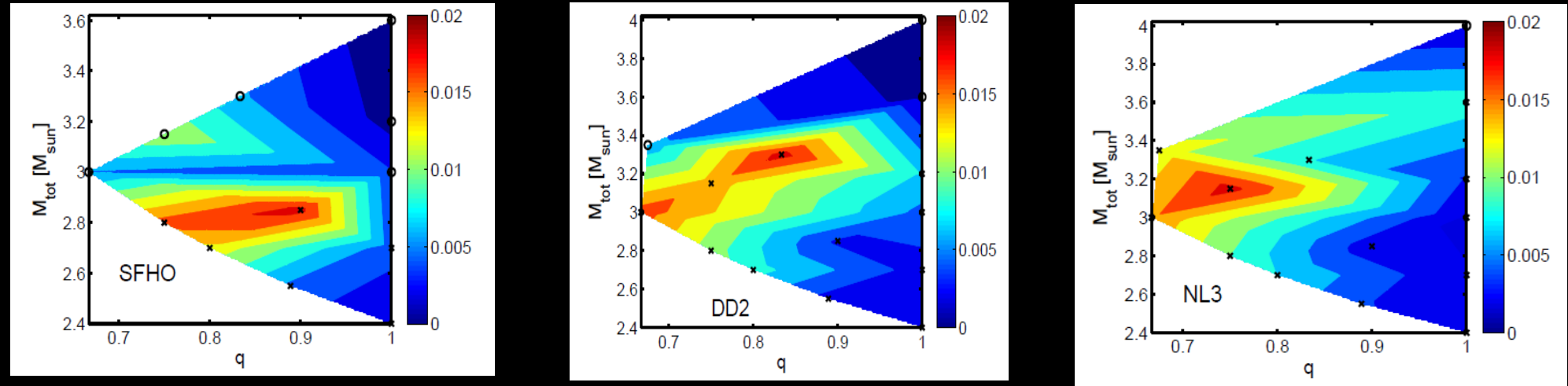


Bauswein et al 2013, see also Hotokezaka et al 2013

+ secular ejecta (viscous, neutrino)

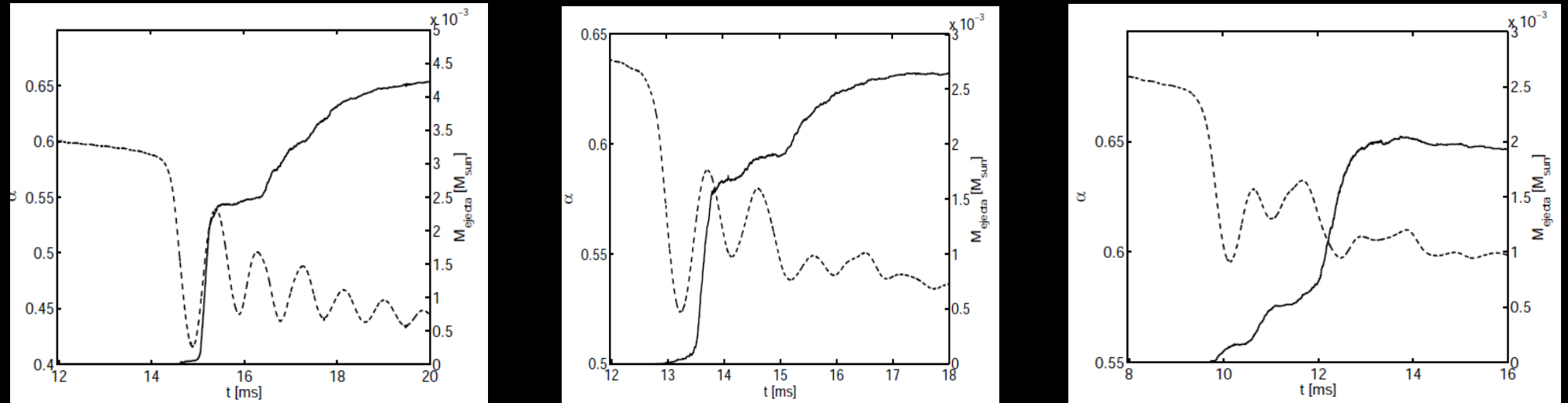
Compilation in Cote et al 2018

Ejecta mass dependencies: binary para.



→ Stiffness →

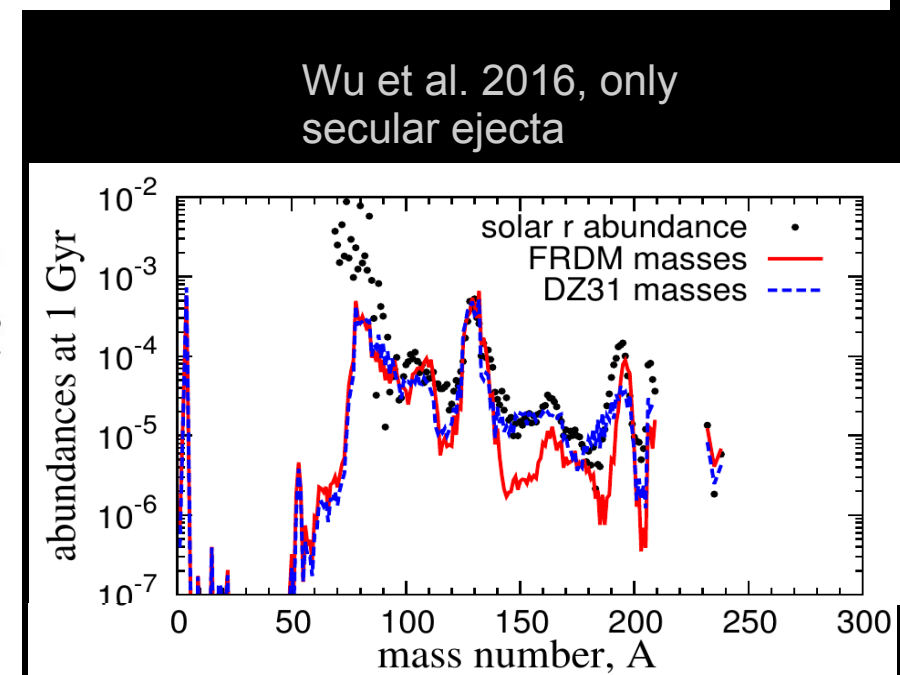
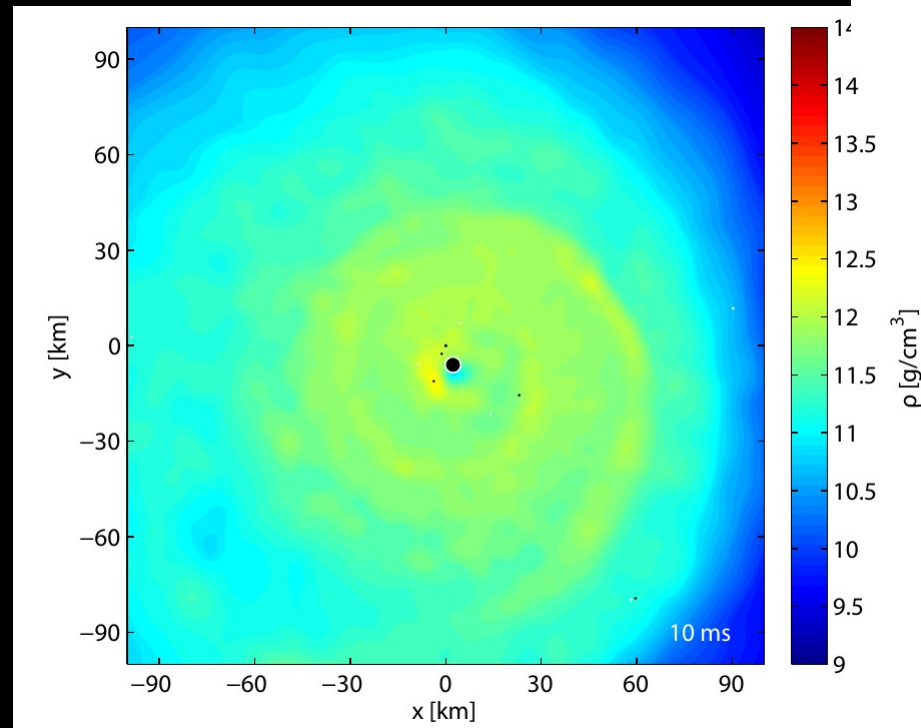
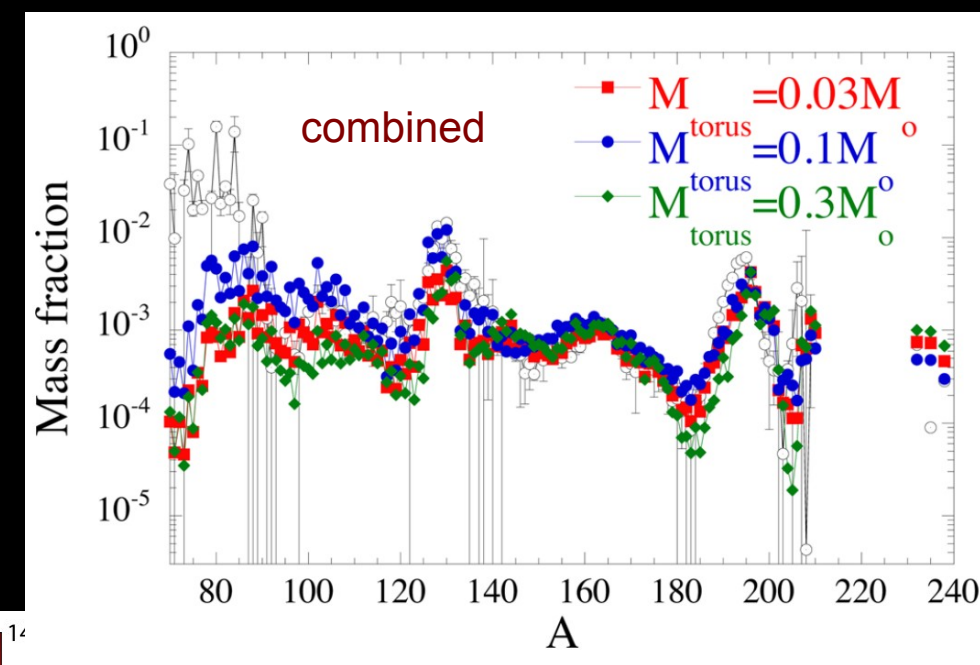
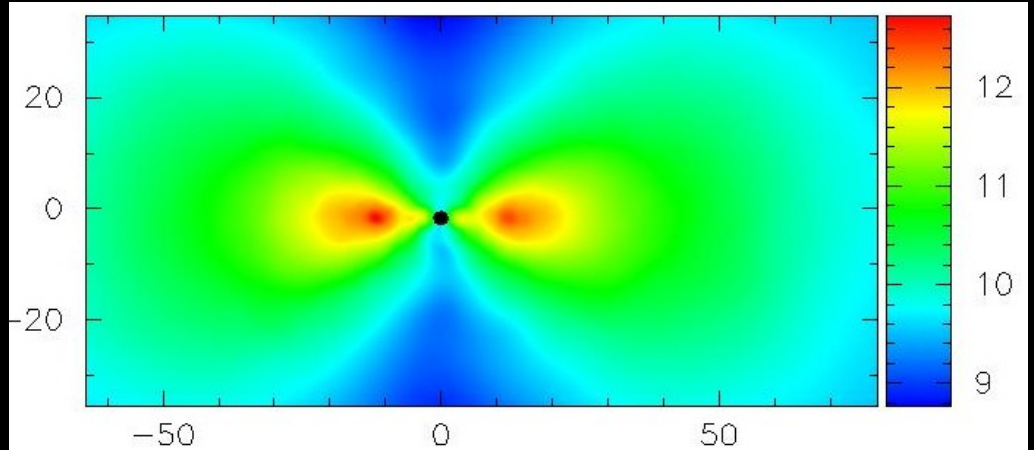
understandable by different dynamics / impact velocity / postmerger oscillations



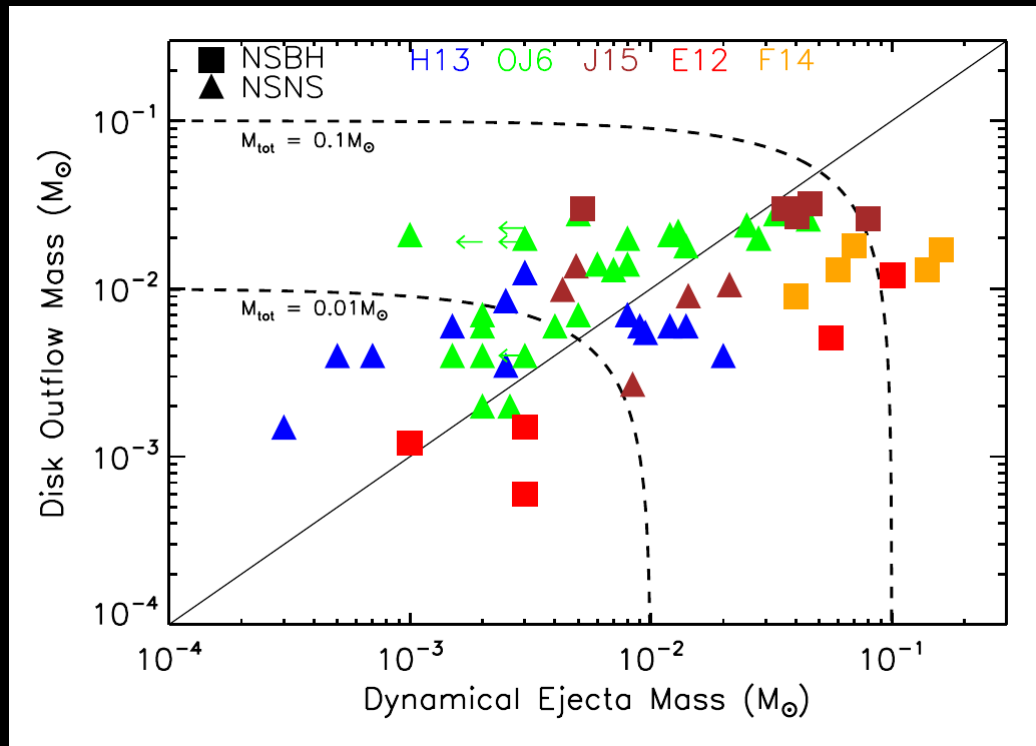
Central lapse α traces remnant compactness / oscillations / dynamics (dashed lines)

Secular and dynamical ejecta

Just et al. 2015



Secular ejecta

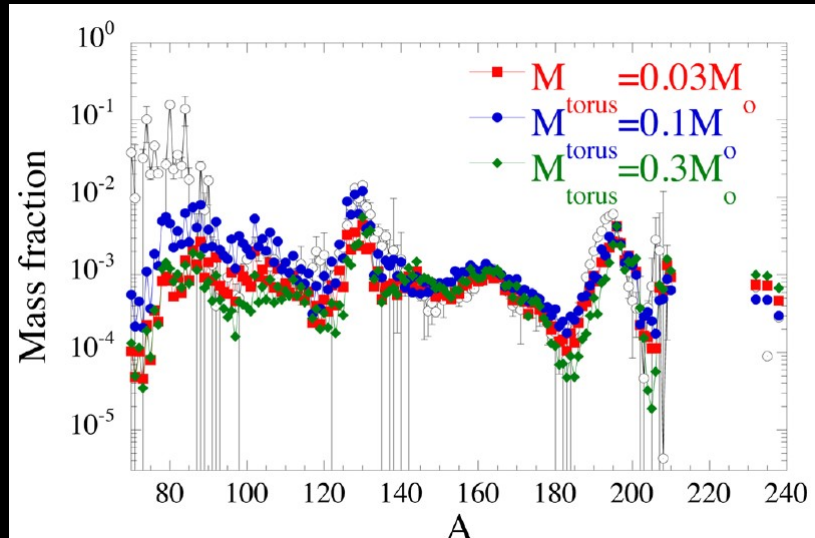


Wu et al. 2016

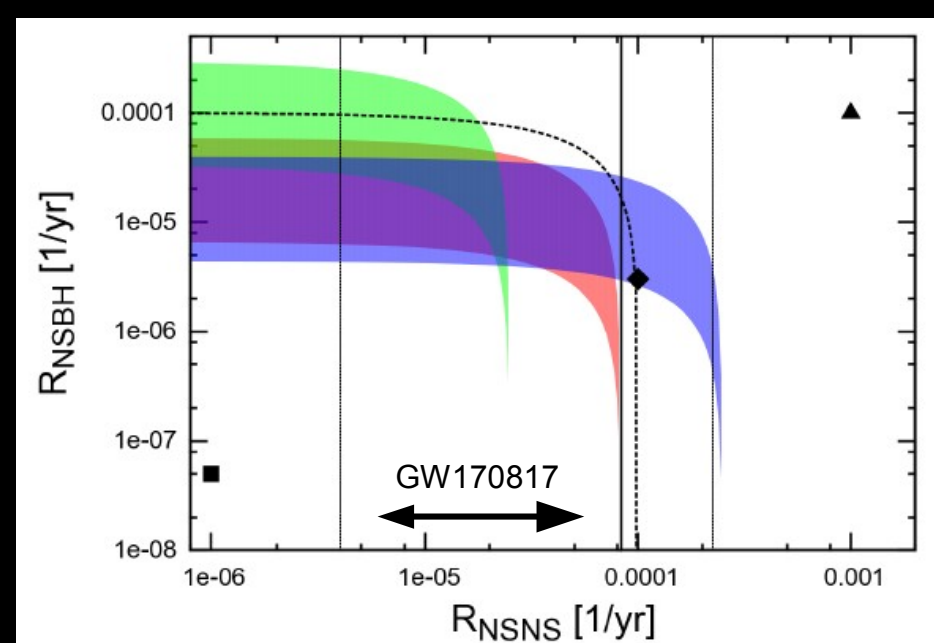
Typically several per cent of disk mass ejected (e.g. Fernandez et al. 2014, Perego et al. 2014, Just et al 2015) → production of light and heavy r-process elements, contributing to em counterpart

Interpretation - implications

- ▶ heating and derived opacities are compatible with r-processing ejecta !!!
(not surprising for a theorist, see earlier work on r-process and em counterparts)
- ▶ Ejecta velocities and masses in ballpark of simulation results (\rightarrow later)
- ▶ Derived ejecta masses are compatible with mergers being the main source of heavy r-process elements in the Universe
 \rightarrow overall strong evidence that NS mergers play a prominent role for heavy element formation



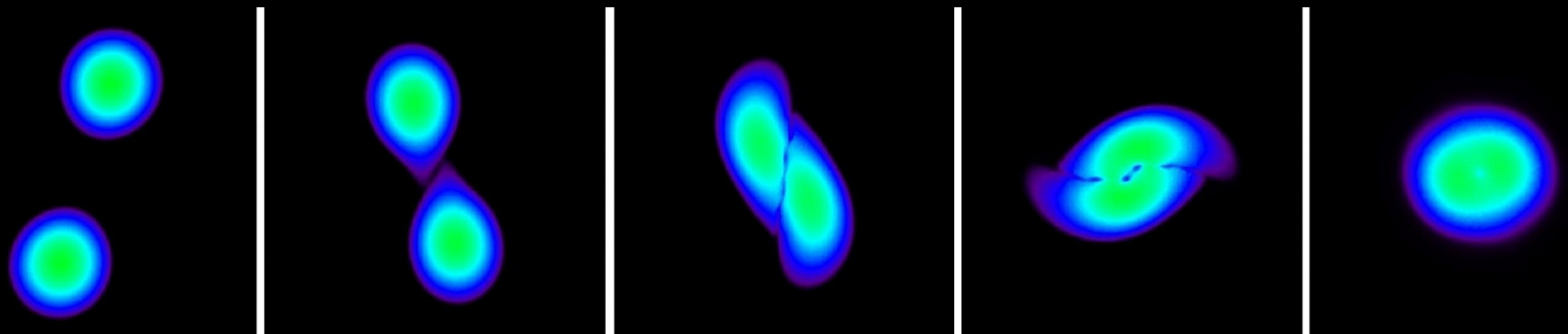
Just et al. 2015



Bauswein et al. 2014

EoS / NS constraints

Finite-size effects during late inspiral



See Lattimer's talk

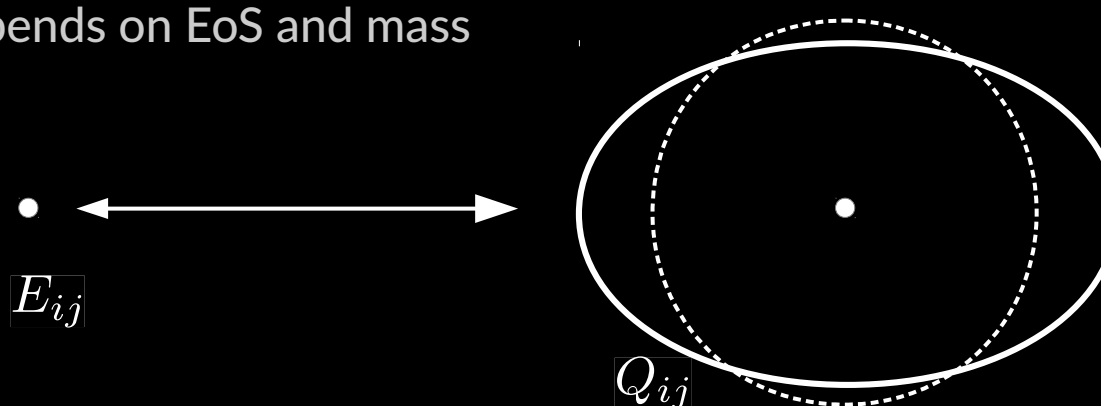
Description of tidal effects during inspiral

- ▶ Tidal field E_{ij} of one star induces change of quadrupole moment Q_{ij} of other component
- ▶ Changed quadrupole moment affects GW signal, especially phase evolution
→ inspiral faster compared to point-particle inspiral
- ▶ Strength of induced quadrupole moment depends on NS structure / EoS:

$$Q_{ij} = -\lambda(M) E_{ij}$$

$$\lambda(M) = \frac{2}{3} k_2(M) R^5$$

- ▶ Tidal deformability depends on radius (clear – smaller stars are harder to deform) and “Love number” k_2 (~“TOV” properties)
- ▶ k_2 also depends on EoS and mass

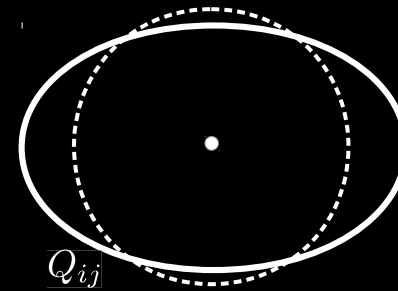


Tidal effects during the inspiral

- ▶
$$\lambda(M) = \frac{2}{3}k_2(M)R^5$$
- ▶ Compute tidal deformability for given EoS and mass:
 - radius via TOV (easy)
 - Love number k_2 can be computed in a similar manner

→ essentially an extended TOV system, i.e. system of ordinary differential equations that can be solved as initial value problem

Love number



$l=2$ metric perturbation of spherical star
 → encoded in $H(r)$, $K(r)$ (depend only on r !!!)

$$\begin{aligned} ds^2 = & -e^{2\Phi(r)} [1 + H(r)Y_{20}(\theta, \varphi)] dt^2 \\ & + e^{2\Lambda(r)} [1 - H(r)Y_{20}(\theta, \varphi)] dr^2 \\ & + r^2 [1 - K(r)Y_{20}(\theta, \varphi)] (d\theta^2 + \sin^2 \theta d\varphi^2) \end{aligned}$$

Solve standard TOV system:

$$\begin{aligned} e^{2\Lambda} &= \left(1 - \frac{2m_r}{r}\right)^{-1}, \\ \frac{d\Phi}{dr} &= -\frac{1}{\epsilon + p} \frac{dp}{dr}, \\ \frac{dp}{dr} &= -(\epsilon + p) \frac{m_r + 4\pi r^3 p}{r(r - 2m_r)}, \\ \frac{dm_r}{dr} &= 4\pi r^2 \epsilon. \end{aligned}$$

And integrate in parallel:

$$\begin{aligned} \frac{dH}{dr} &= \beta \\ \frac{d\beta}{dr} &= 2 \left(1 - 2\frac{m_r}{r}\right)^{-1} H \left\{ -2\pi [5\epsilon + 9p + f(\epsilon + p)] \right. \\ &\quad \left. + \frac{3}{r^2} + 2 \left(1 - 2\frac{m_r}{r}\right)^{-1} \left(\frac{m_r}{r^2} + 4\pi r p\right)^2 \right\} \\ &\quad + \frac{2\beta}{r} \left(1 - 2\frac{m_r}{r}\right)^{-1} \left\{ -1 + \frac{m_r}{r} + 2\pi r^2 (\epsilon - p) \right\} \end{aligned}$$

Lecture by Stergioulas

→ system of ordinary differential equations that can be solved as initial value problem

Love number and tidal deformability

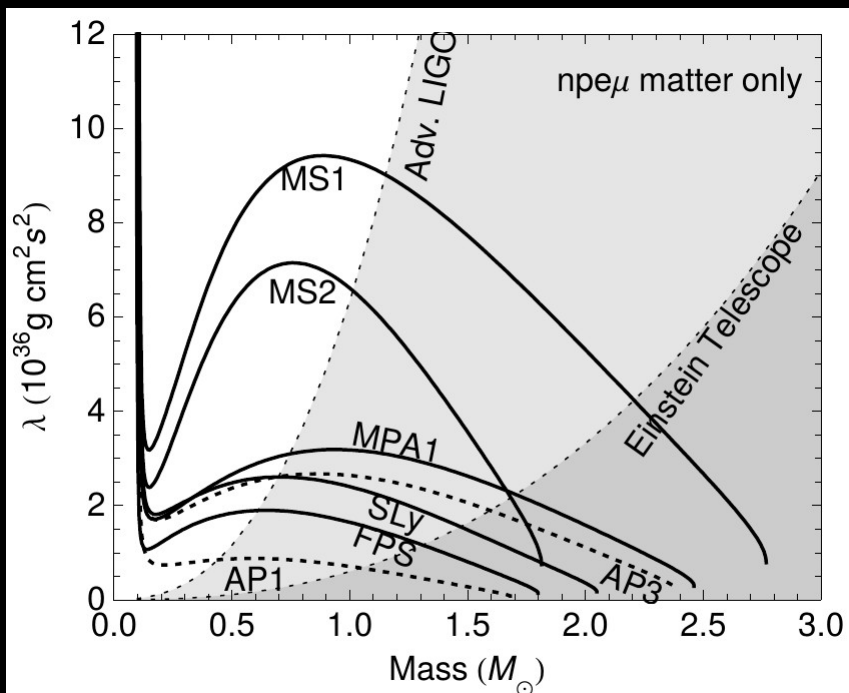
- ▶ Love number given by:

$$k_2 = \frac{8C^5}{5}(1 - 2C)^2[2 + 2C(y - 1) - y] \\ \times \left\{ 2C[6 - 3y + 3C(5y - 8)] + 4C^3[13 - 11y + C(3y - 2) + 2C^2(1 + y)] + 3(1 - 2C)^2[2 - y + 2C(y - 1)] \ln(1 - 2C) \right\}^{-1},$$

with $y = \frac{R\beta(R)}{H(R)}$

Compactness C, radius R
Mass m

$$C = m/R$$



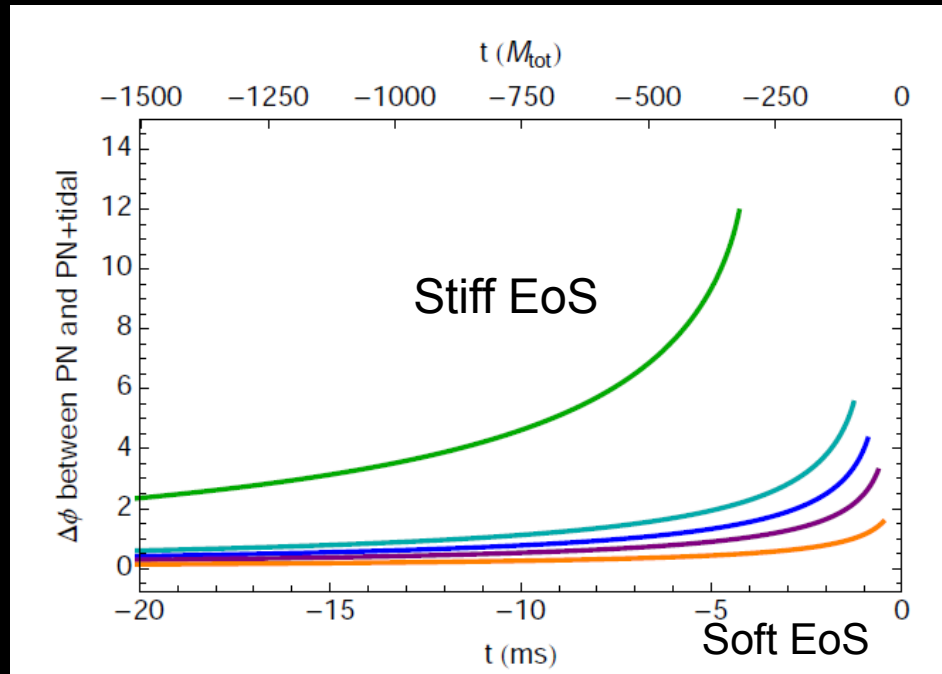
$$\lambda(M) = \frac{2}{3} k_2(M) R(M)^5$$

- Larger/lighter stars have larger tidal deformability
- Stiffer EoS have have deformability
- discern different EoSs (for known mass)

Hinderer et al. 2010

Inspiral

- ▶ Orbital phase evolution affected by tidal deformability – only during last orbits before merging
- ▶ Inspiral accelerated compared to point-particle inspiral for larger Lambda
- ▶ Difference in phase between NS merger and point-particle inspiral:



e.g. Read et al. 2013

EoS impact measured by tidal deformability

$$\Lambda(M) = \frac{2}{3}k_2(M) \left(\frac{c^2 R}{G M} \right)^5$$

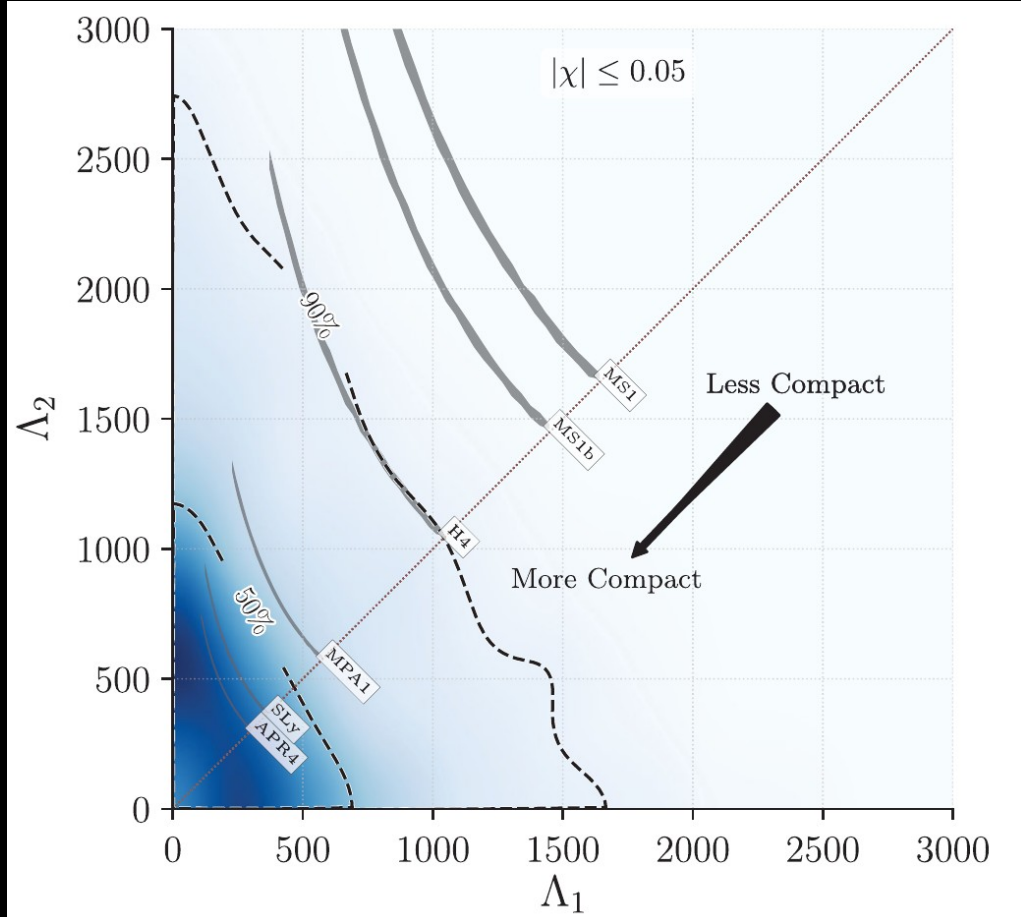
↑
Merger time of point particle

Challenge: construct faithful templates for data analysis

Measurement

- ▶ $\Lambda < \sim 800$
→ Means that very stiff EoSs are excluded
- ▶ For other priors/assumptions even tighter constraints
- ▶ Better constraints expected in future as sensitivity increases

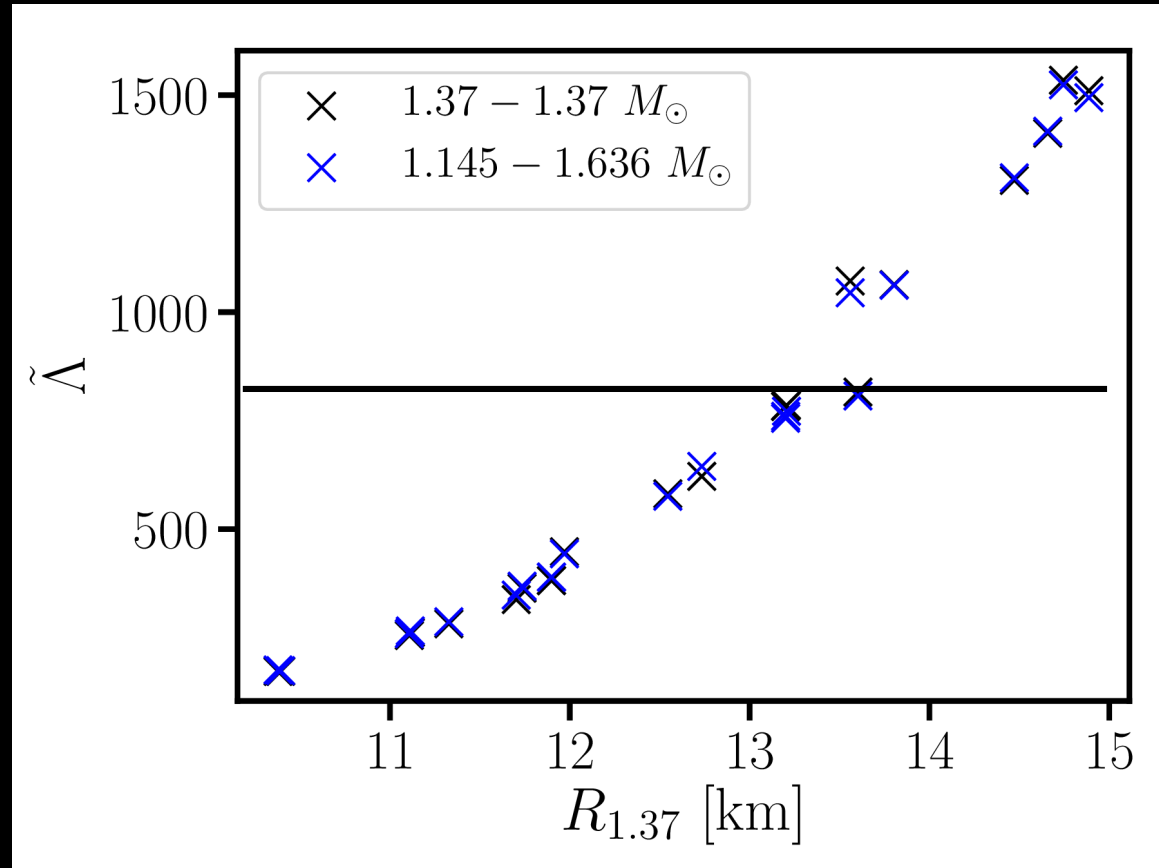
$$\tilde{\Lambda} = \frac{16}{13} \frac{(m_1 + 12m_2)m_1^4\Lambda_1 + (m_2 + 12m_1)m_2^4\Lambda_2}{(m_1 + m_2)^5}$$



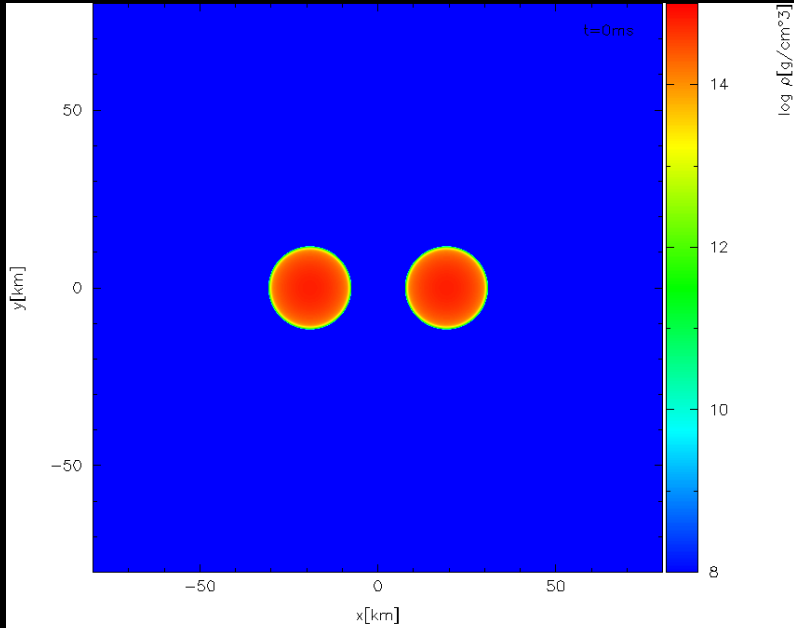
$\tilde{\Lambda} = \Lambda$ for equal-mass binaries !!

Abbott et al. 2017
See also later publications by
Ligo/Virgo collaboration, De et al. 2018

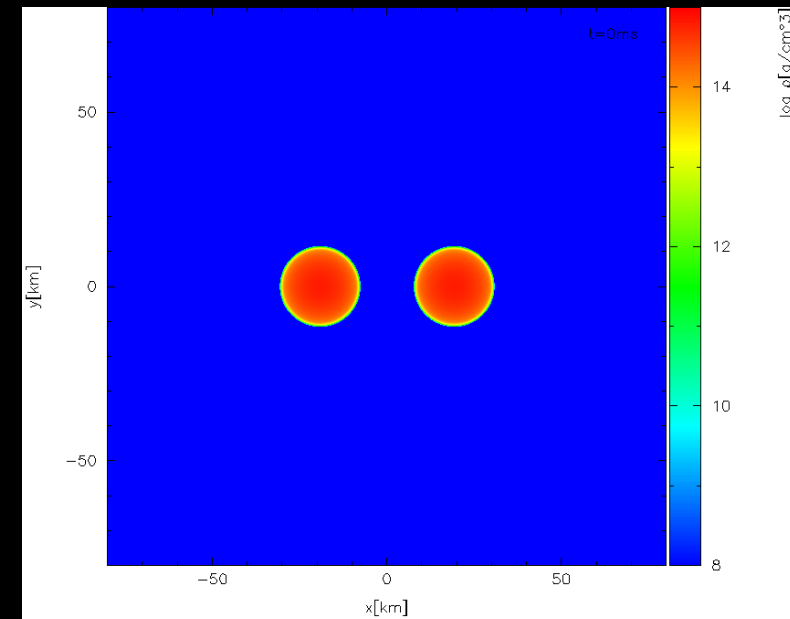
- Combined tidal deformability vs. radius (for constant chirp mass)



→ GW170817 constrains NS radii from above



$$M_{\text{tot}} = 3.4 M_{\odot}$$



$$M_{\text{tot}} = 3.5 M_{\odot}$$

Shen EoS

Collapse behavior: Prompt vs. delayed (/no) BH formation

Relevant for:

EoS constraints through M_{max} measurement

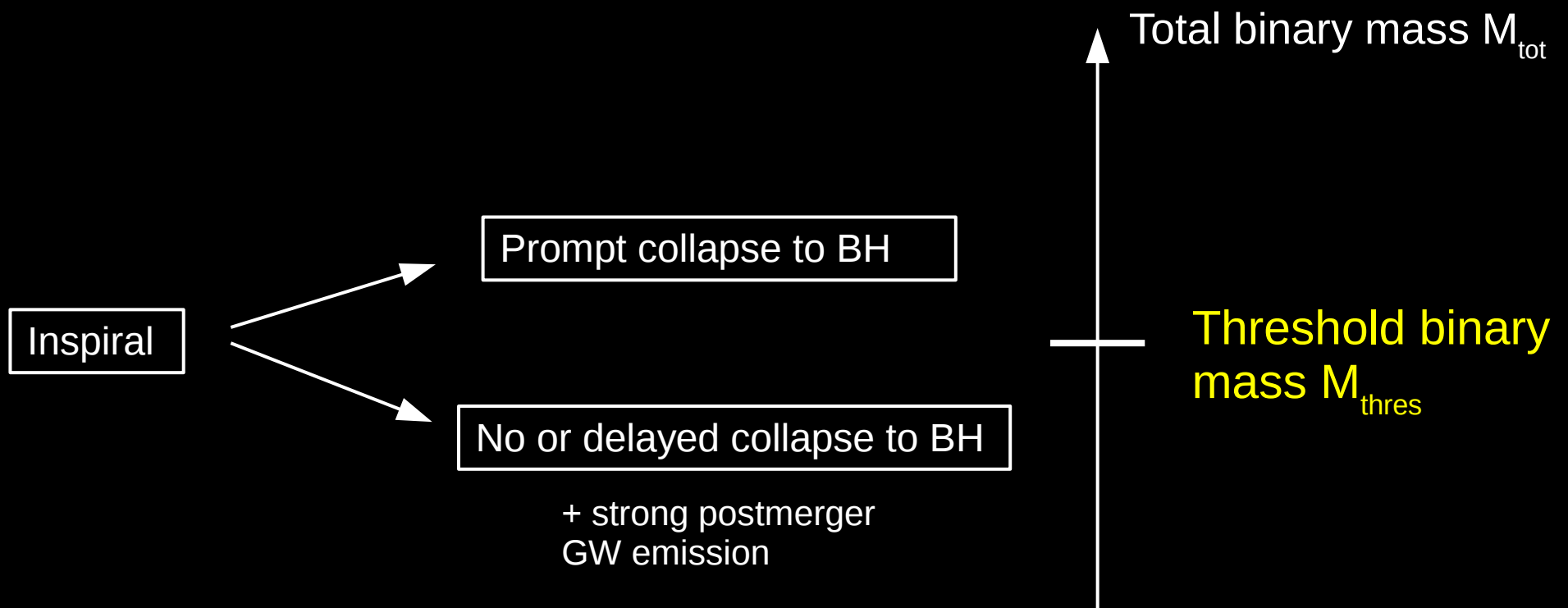
Conditions for short GRBs

Mass ejection

Electromagnetic counterparts powered by thermal emission

And NS radius constraints !!!

Collapse behavior



EoS dependent - somehow M_{max} should play a role

Simulations reveal M_{thres}

TOV properties of nonrotating stars, i.e. EoS characteristics

Merger property from simulations

EoS	M_{max} (M_{\odot})	R_{max} (km)	C_{max}	$R_{1.6}$ (km)	M_{thres} (M_{\odot})
NL3 [37,38]	2.79	13.43	0.307	14.81	3.85
GS1 [39]	2.75	13.27	0.306	14.79	3.85
LS375 [40]	2.71	12.34	0.325	13.71	3.65
DD2 [38,41]	2.42	11.90	0.300	13.26	3.35
Shen [42]	2.22	13.12	0.250	14.46	3.45
TM1 [43,44]	2.21	12.57	0.260	14.36	3.45
SFHX [45]	2.13	10.76	0.292	11.98	3.05
GS2 [46]	2.09	11.78	0.262	13.31	3.25
SFHO [45]	2.06	10.32	0.294	11.76	2.95
LS220 [40]	2.04	10.62	0.284	12.43	3.05
TMA [44,47]	2.02	12.09	0.247	13.73	3.25
IUF [38,48]	1.95	11.31	0.255	12.57	3.05

Smooth particle hydrodynamics + conformal flatness

Bauswein et al. 2013

Threshold binary mass

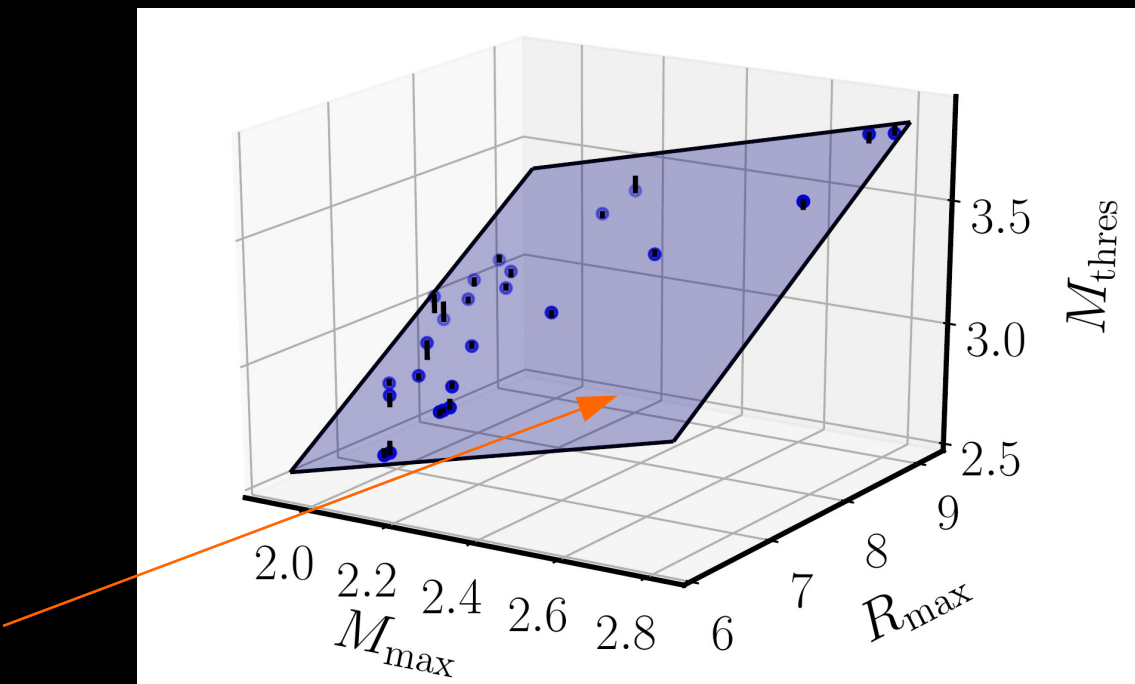
- ▶ Empirical relation from simulations with different M_{tot} and EoS
- ▶ Fits (to good accuracy):

$$M_{\text{thres}} = M_{\text{thres}}(M_{\text{max}}, R_{\text{max}}) = \left(-3.38 \frac{GM_{\text{max}}}{c^2 R_{\text{max}}} + 2.43 \right) M_{\text{max}}$$

$$M_{\text{thres}} = M_{\text{thres}}(M_{\text{max}}, R_{1.6}) = \left(-3.6 \frac{GM_{\text{max}}}{c^2 R_{1.6}} + 2.38 \right) M_{\text{max}}$$

- ▶ Both better than $0.06 M_{\text{sun}}$

Parameter space excluded by causality

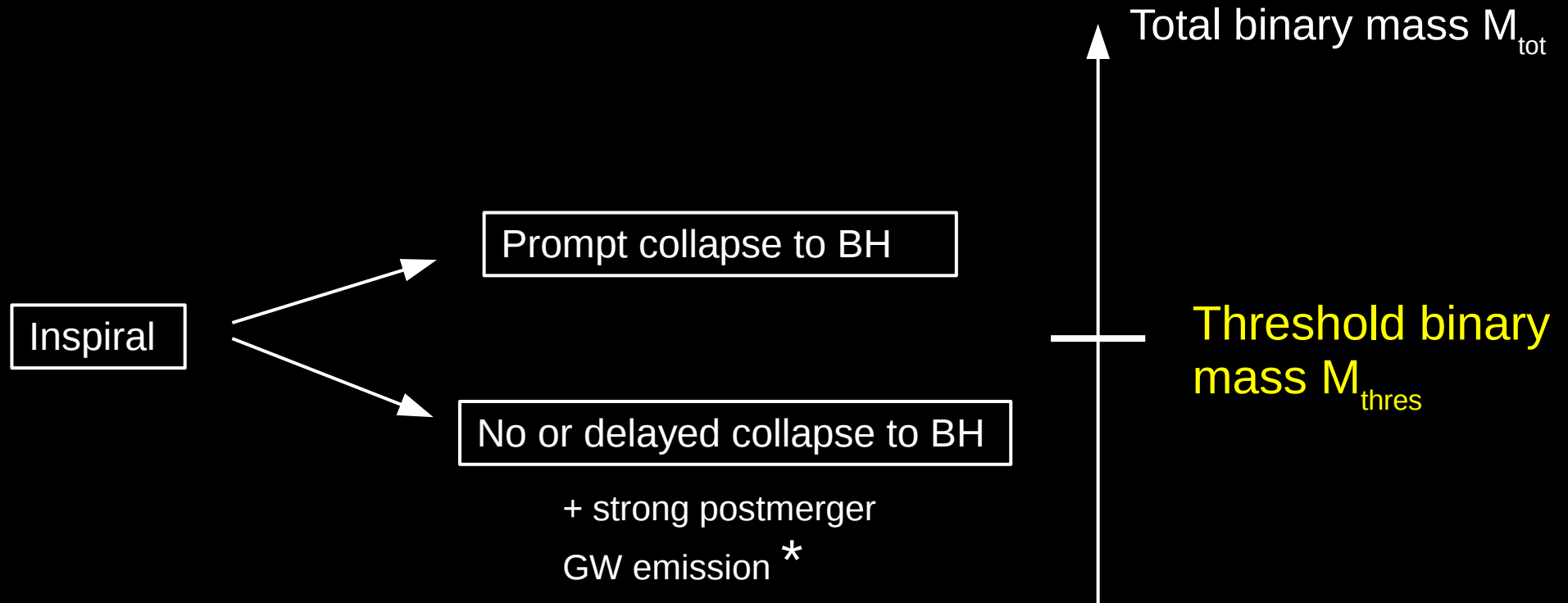


EoS constraints from GW170817*

→ lower bound on NS radii

* See also Margalit & Metzger 2017, Shibata et al. 2017, Rezzolla et al. 2018, Radice et al. 2018, Ruiz & Shapiro 2018, ... for other EoS constraints in the context of GW170817

Collapse behavior



M_{thres} EoS dependent - somehow M_{max} should play a role

A simple but robust NS radius constraint from GW170817

- ▶ High ejecta mass inferred from electromagnetic transient
 - provides strong support for a delayed/no collapse in GW170817
 - even asymmetric mergers that directly collapse do not produce such massive ejecta

Reference	$m_{\text{dyn}} [M_{\odot}]$	$m_w [M_{\odot}]$
Abbott et al. (2017a)	0.001 – 0.01	–
Arcavi et al. (2017)	–	0.02 – 0.025
Cowperthwaite et al. (2017)	0.04	0.01
Chornock et al. (2017)	0.035	0.02
Evans et al. (2017)	0.002 – 0.03	0.03 – 0.1
Kasen et al. (2017)	0.04	0.025
Kasliwal et al. (2017b)	> 0.02	> 0.03
Nicholl et al. (2017)	0.03	–
Perego et al. (2017)	0.005 – 0.01	$10^{-5} – 0.024$
Rosswog et al. (2017)	0.01	0.03
Smartt et al. (2017)	0.03 – 0.05	0.018
Tanaka et al. (2017a)	0.01	0.03
Tanvir et al. (2017)	0.002 – 0.01	0.015
Troja et al. (2017)	0.001 – 0.01	0.015 – 0.03

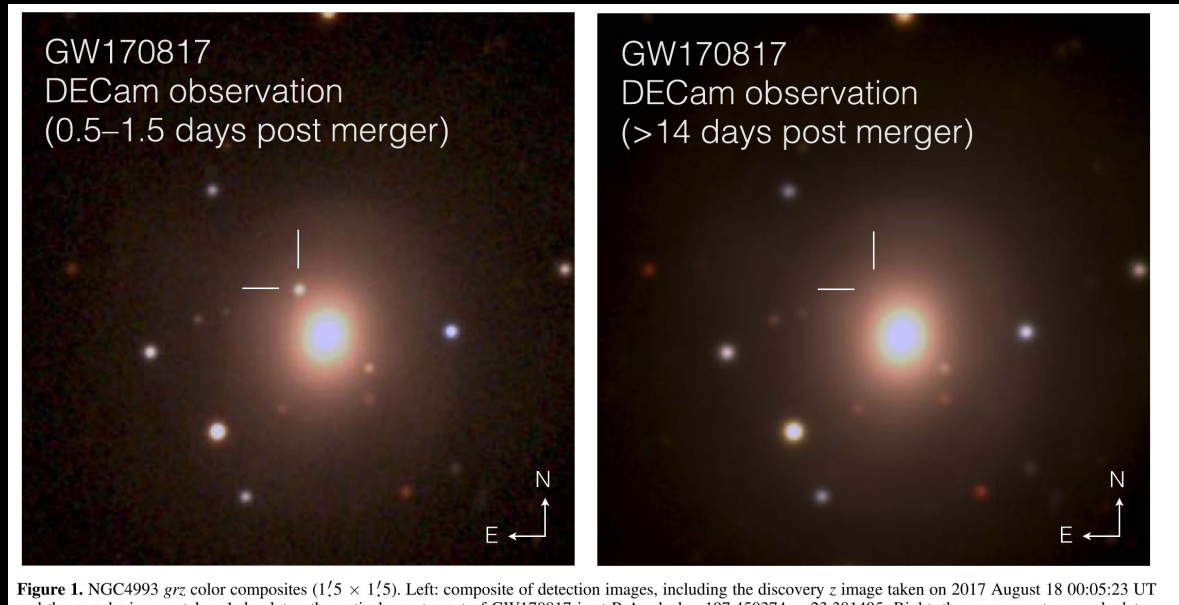
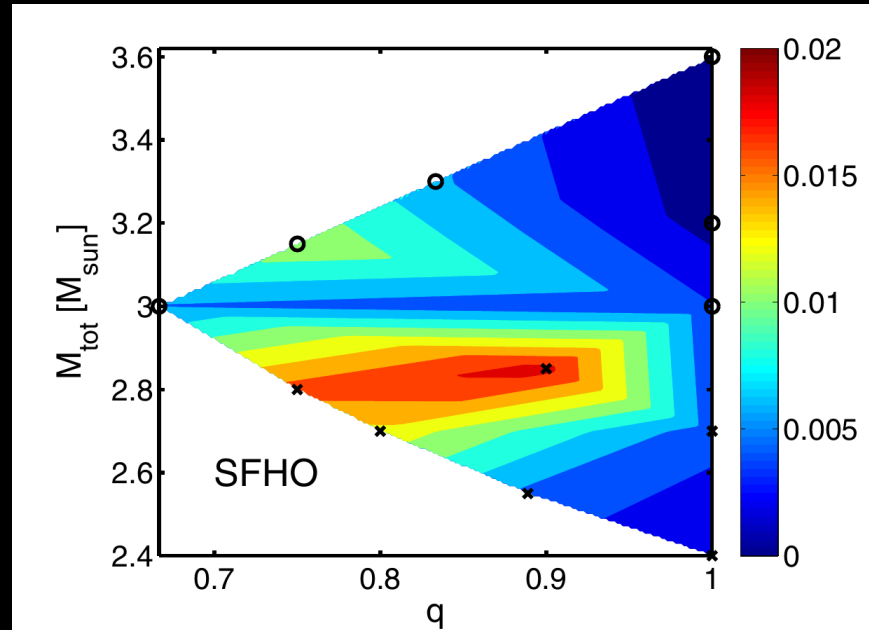
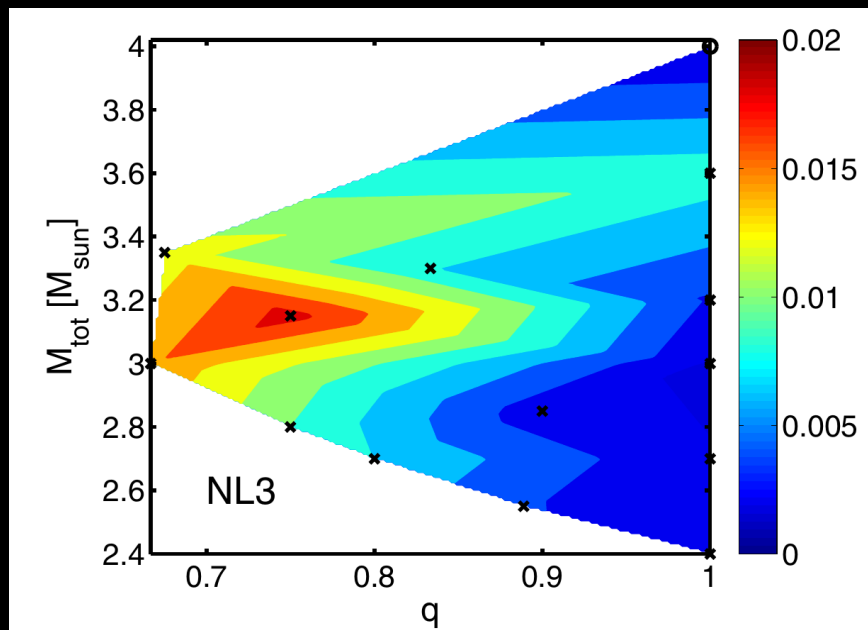
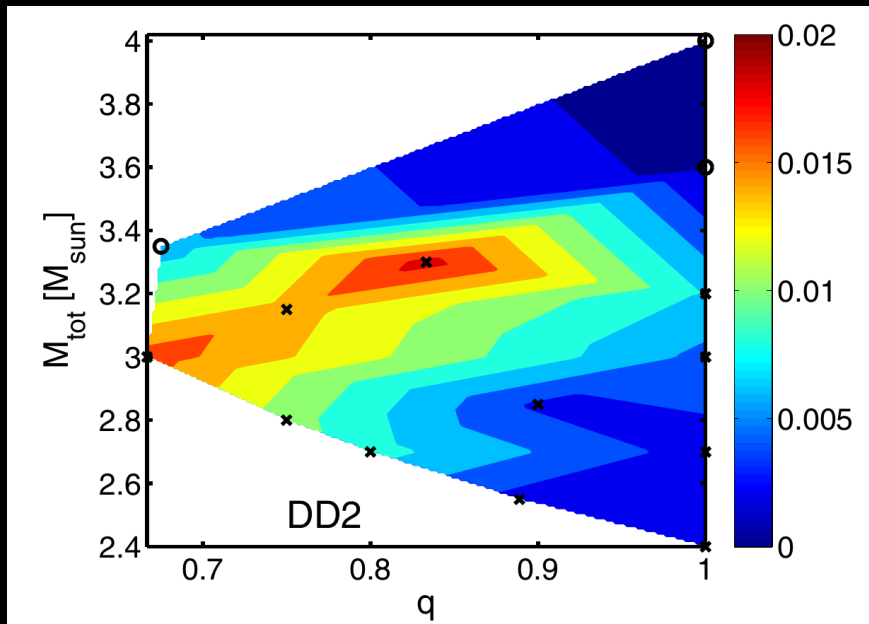


Figure 1. NGC4993 grz color composites ($1/5 \times 1/5$). Left: composite of detection images, including the discovery z image taken on 2017 August 18 00:05:23 UT and the g and r images taken 1 day later; the optical counterpart of GW170817 is at R.A., decl. = $197.450374, -23.381495$. Right: the same area two weeks later.

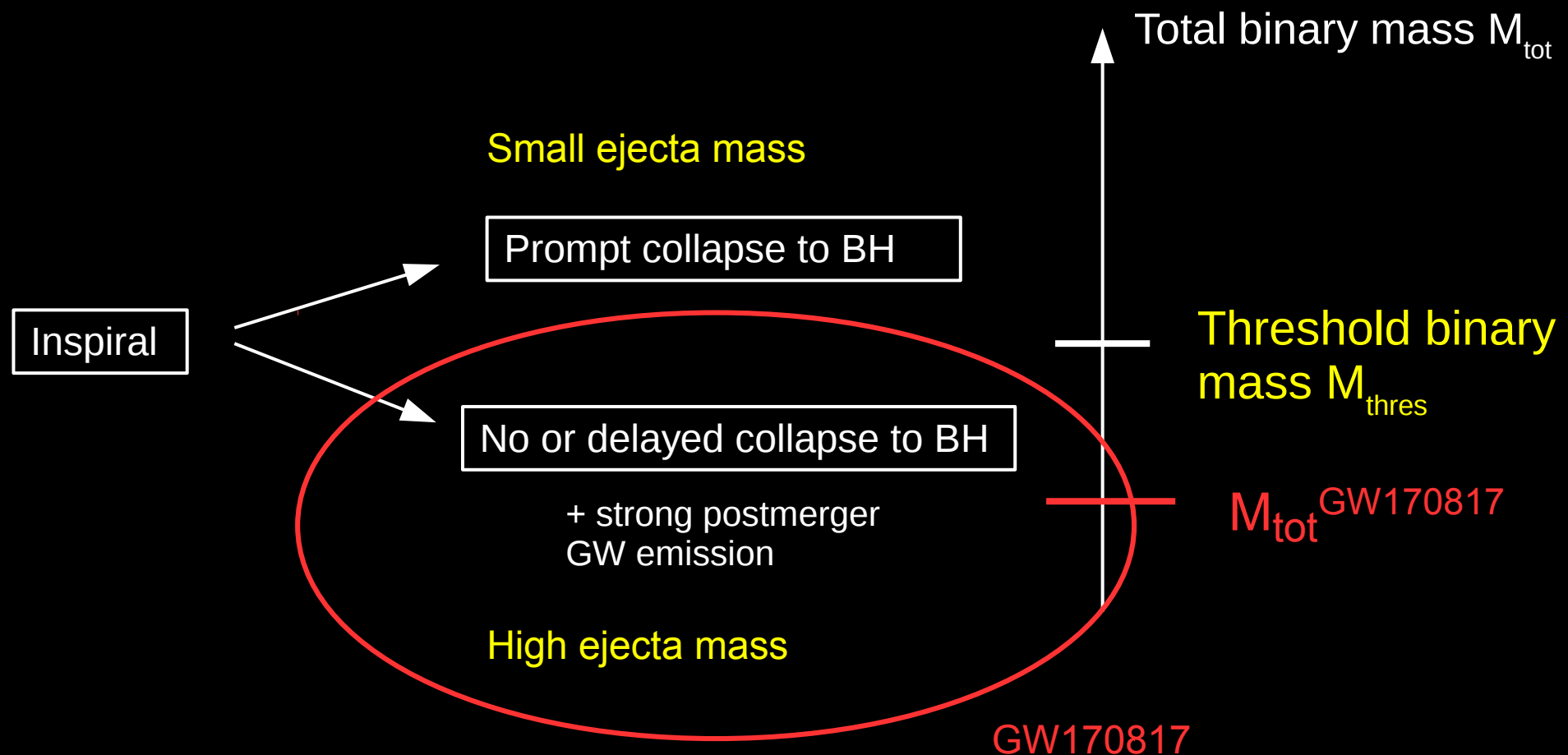
Soares-Santos et al 2017

- ▶ Ejecta masses depend on EoS and binary masses
- ▶ Note: high mass points already to soft EoS (tentatively/qualitatively)
- ▶ Prompt collapse leads to reduced ejecta mass
- ▶ Light curve depends on ejecta mass:
→ 0.02 - 0.05 M_{sun} point to delayed collapse
- ▶ Note: here only dynamical ejecta

Only dynamical ejecta



Collapse behavior



(1) If GW170817 was a delayed (/no) collapse:

$$M_{\text{thres}} > M_{\text{tot}}^{\text{GW170817}}$$

(2) Recall: empirical relation for threshold binary mass for prompt collapse:

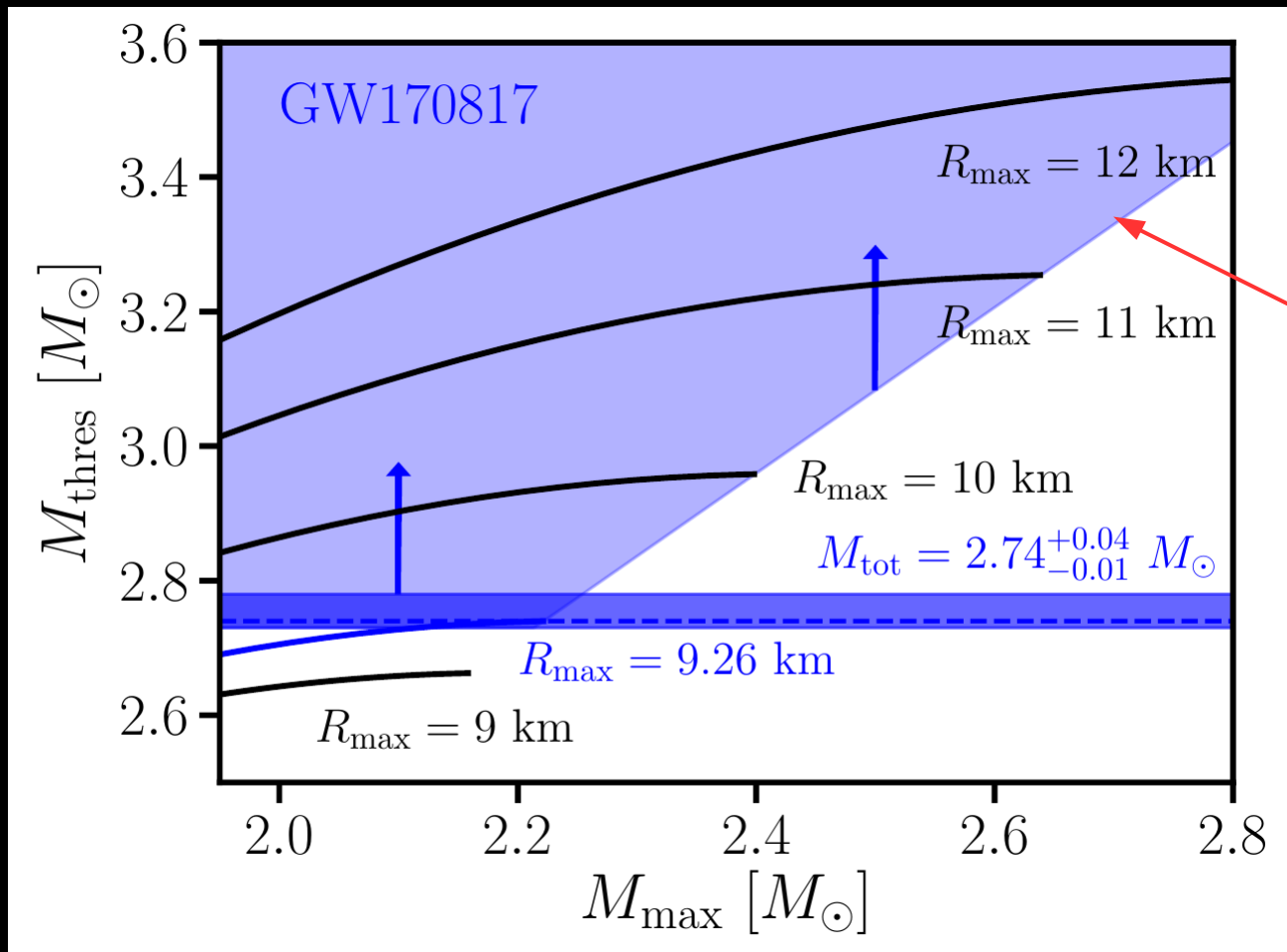
$$M_{\text{thres}} = \left(-3.38 \frac{G M_{\text{max}}}{c^2 R_{\text{max}}} + 2.43 \right) M_{\text{max}} > 2.74 M_{\odot} \quad (\text{with } M_{\text{max}}, R_{\text{max}} \text{ unknown})$$

(3) Causality: speed of sound $v_S \leq c$ $\Rightarrow M_{\text{max}} \leq \frac{1}{2.82} \frac{c^2 R_{\text{max}}}{G}$

► Putting things together:

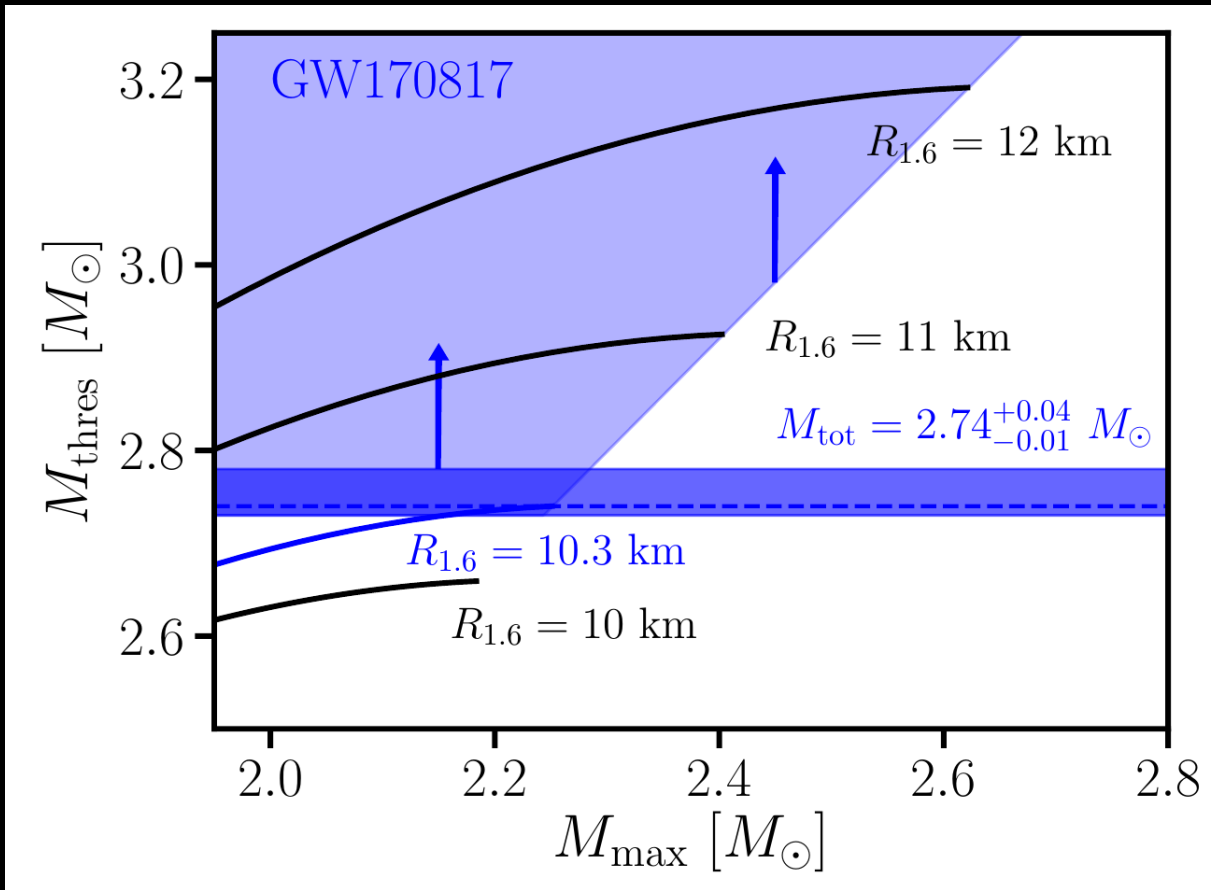
$$M_{\text{tot}}^{\text{GW170817}} \leq \left(-3.38 \frac{G M_{\text{max}}}{c^2 R_{\text{max}}} + 2.43 \right) M_{\text{max}} \leq \left(-\frac{3.38}{2.82} + 2.43 \right) \frac{1}{2.82} \frac{c^2 R_{\text{max}}}{G}$$

→ Lower limit on NS radius



$$M_{\text{thres}} = \left(-3.38 \frac{GM_{\text{max}}}{c^2 R_{\text{max}}} + 2.43 \right) M_{\text{max}}$$

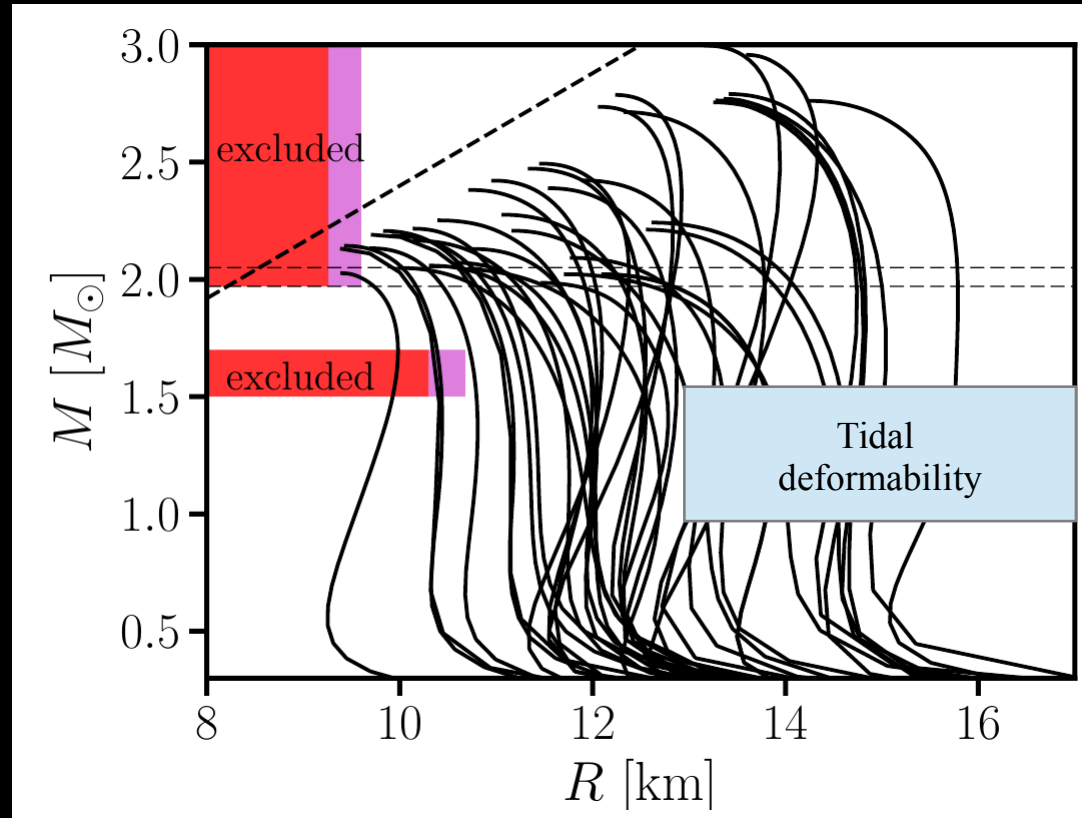
$$M_{\text{thres}} \geq 1.2 M_{\text{max}}$$



$$M_{\text{thres}} = \left(-3.6 \frac{G M_{\text{max}}}{c^2 R_{1.6}} + 2.38 \right) M_{\text{max}}$$

$$v_S = \sqrt{\frac{dP}{de}} \leq c \rightarrow M_{\text{max}} \leq \kappa R_{1.6} \Rightarrow M_{\text{thres}} \geq 1.2 M_{\text{max}}$$

NS radius constraint from GW170817



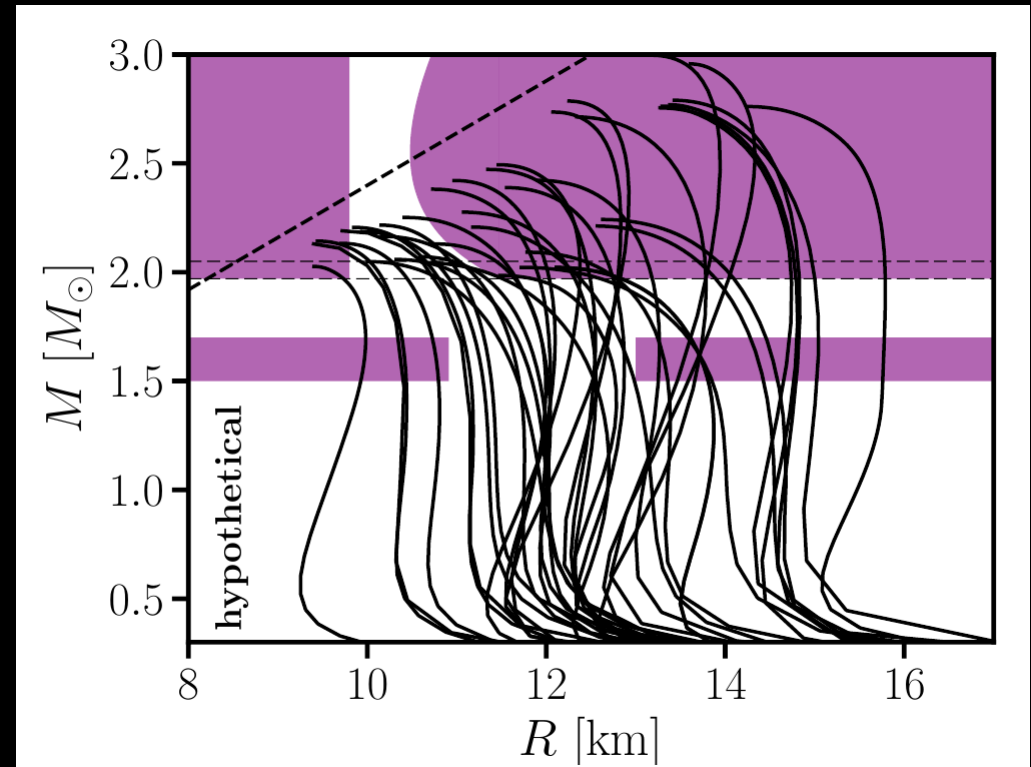
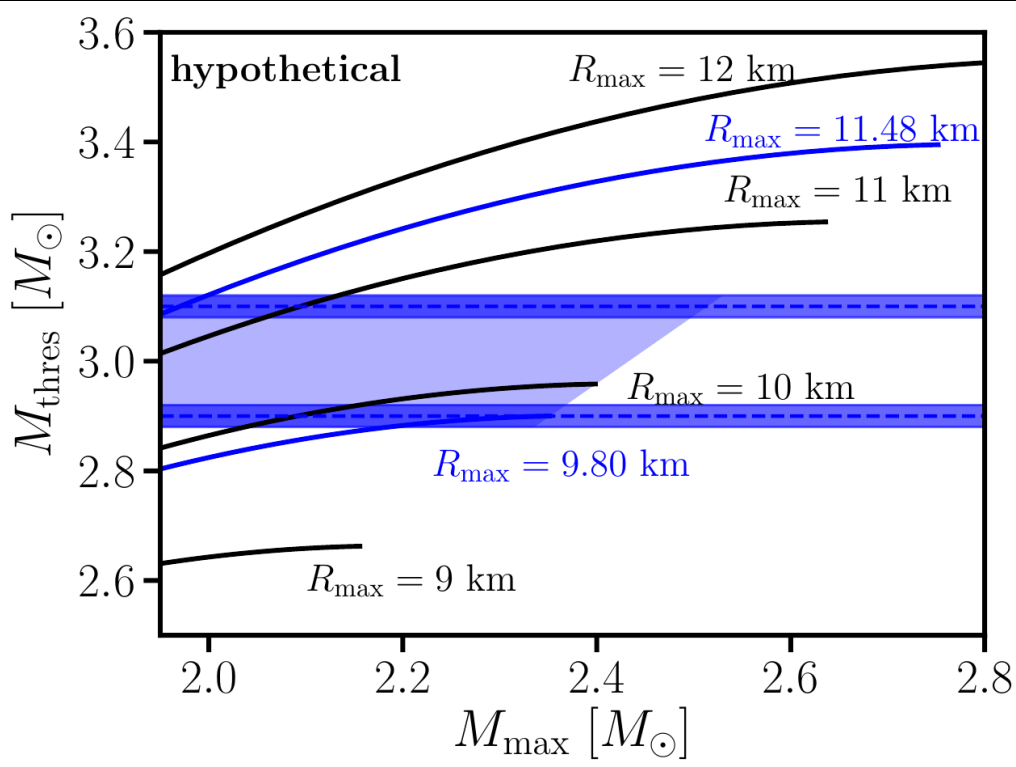
Bauswein et al. 2017

- ▶ $R_{1.6} > 10.7$ km
- ▶ Excludes very soft nuclear matter

Future

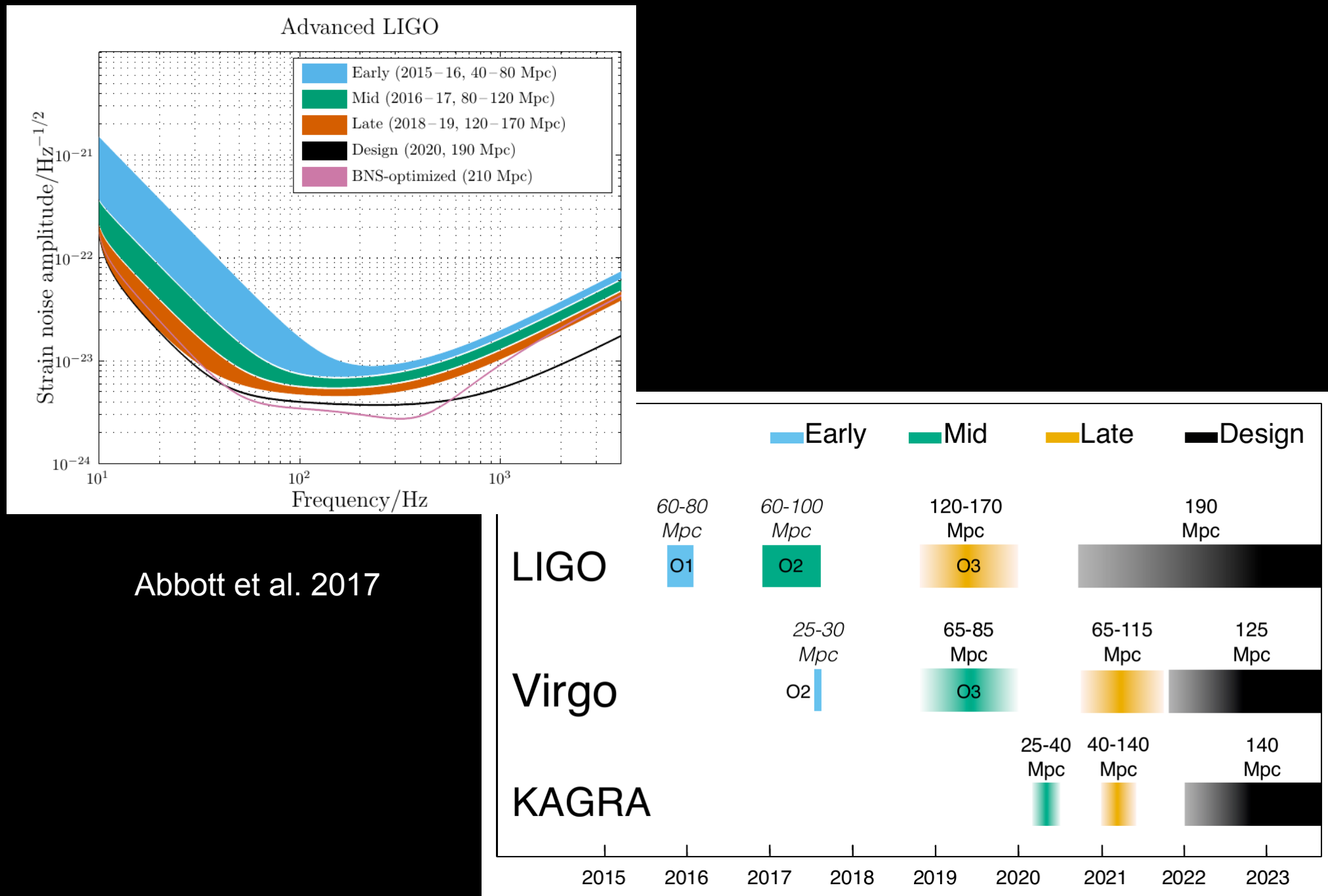
- ▶ Any new detection can be employed if it allows distinction between prompt/delayed collapse
- ▶ With more events in the future our comprehension of em counterparts will grow → more robust discrimination of prompt/delayed collapse events
- ▶ Low-SNR detections sufficient !!! → that's the potential for the future
 - we don't need louder events, but more
 - complimentary to existing ideas for EoS constraints

Future detections (hypothetical discussion)



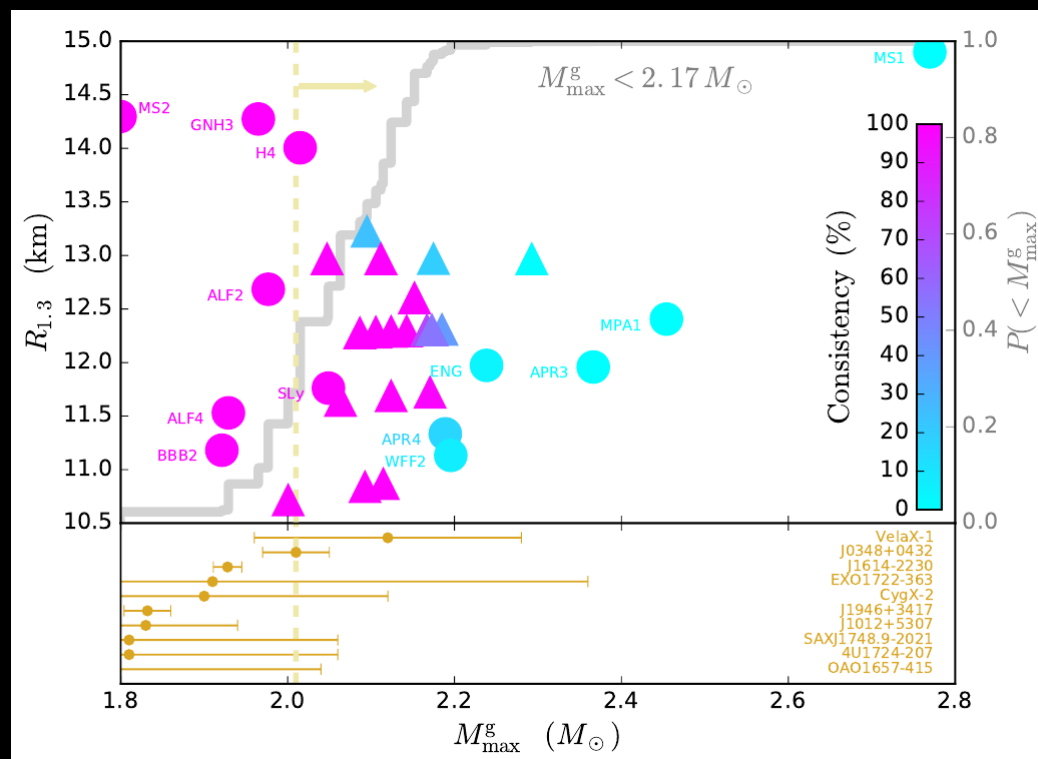
- as more events are observed, bands converge to true M_{thres}
- prompt collapse constrains M_{\max} from above

Future plans



M_{\max} from GW170817

- Arguments: no prompt collapse; no long-lasting pulsar spin-down (too less energy deposition)
- If GW170817 did not form a supramassive NS (rigidly rotating $> M_{\max}$)
→ $M_{\max} < \sim 2.2\text{-}2.4 M_{\odot}$ (relying on some assumption)



Future: Maximum mass

- ▶ Empirical relation

$$M_{\text{thres}} = \left(-3.6 \frac{G M_{\max}}{c^2 R_{1.6}} + 2.38 \right) M_{\max}$$

- ▶ Sooner or later we'll know $R_{1.6}$ (e.g. from postmerger) and M_{thres} (from several events - through presence/absence of postmerger GW emission or em counterpart)

=> direct inversion to get precise estimate of M_{\max}

(see also current estimates e.g. by Margalit & Metzger, Rezzolla et al, Ruiz & Shapiro, Shibata et al., ...)

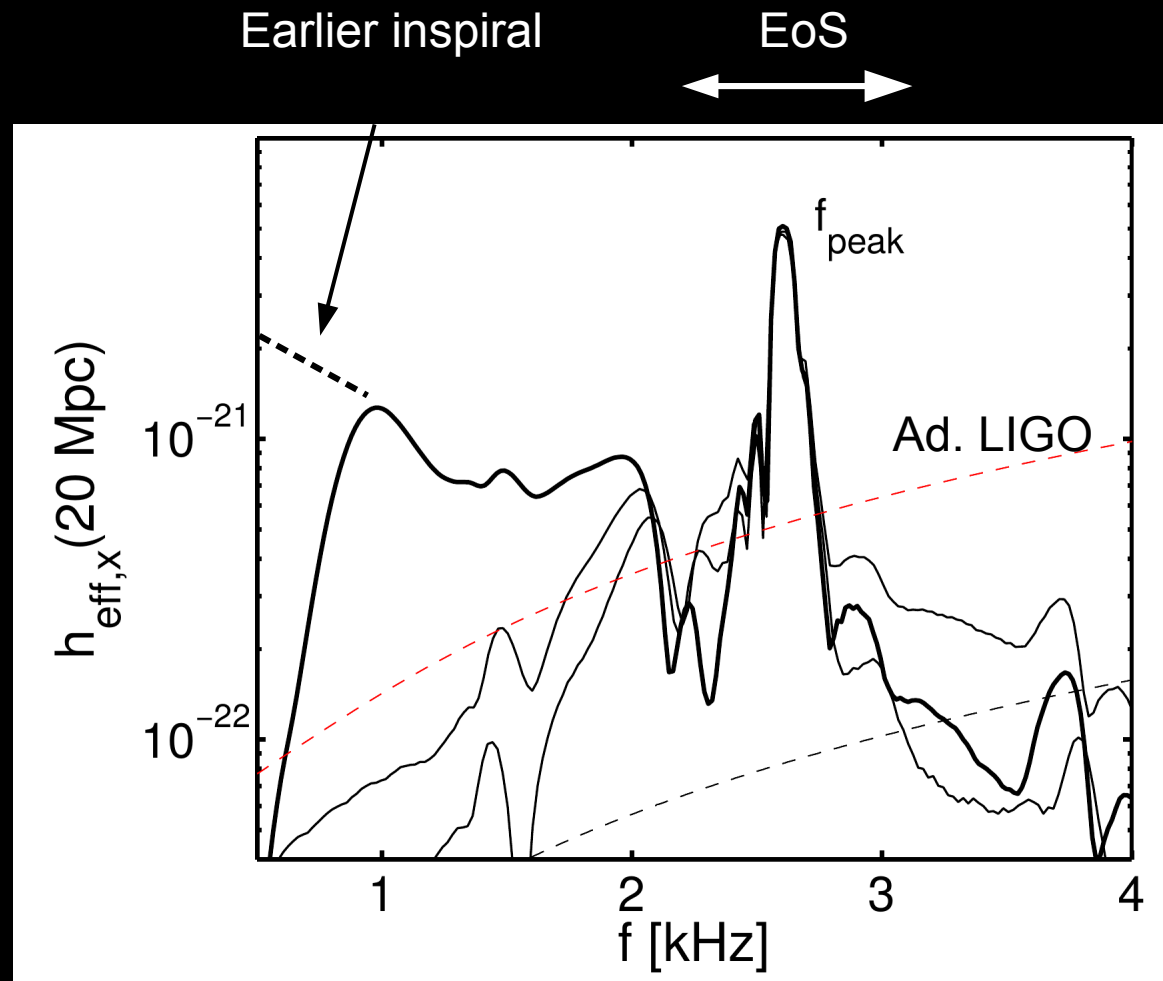
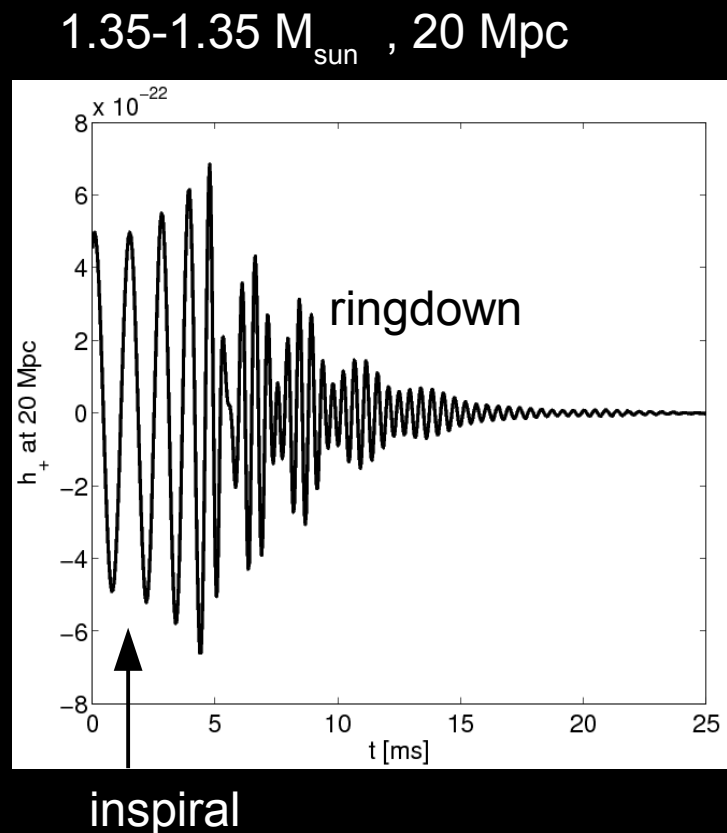
Postmerger GW emission*

(dominant frequency of postmerger phase)

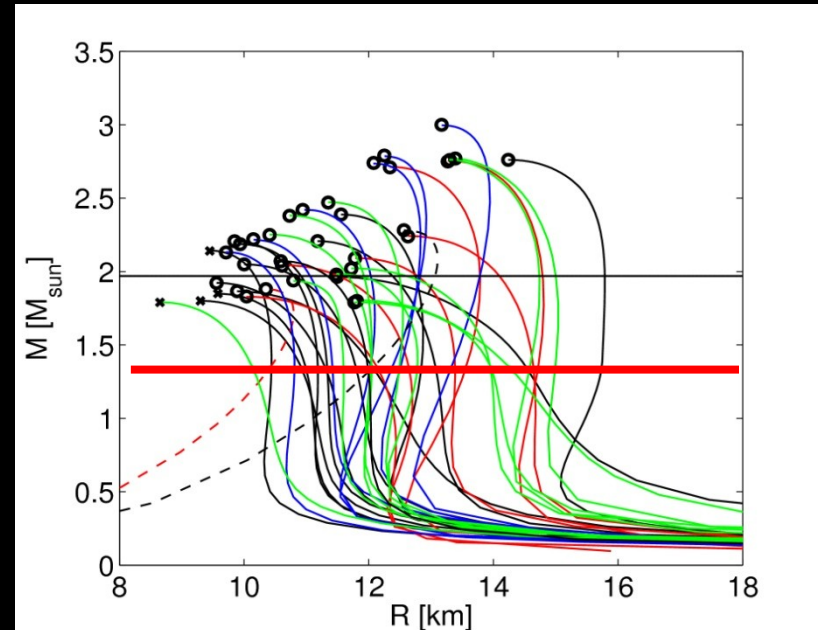
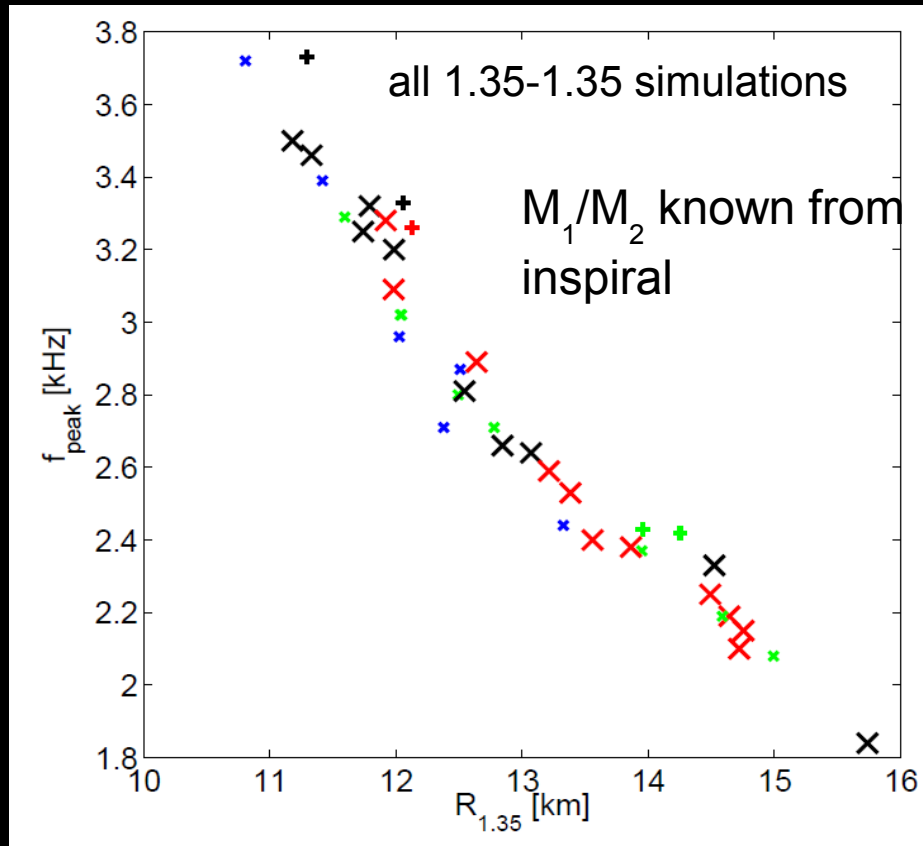
- determine properties of EoS/NSs
- postmerger GW spectrum reveals dynamics

* not detected for GW170817 – expected for current sensitivity and d=40 Mpc
(Abbott et al. 2017)

Postmerger



Gravitational waves - EoS survey



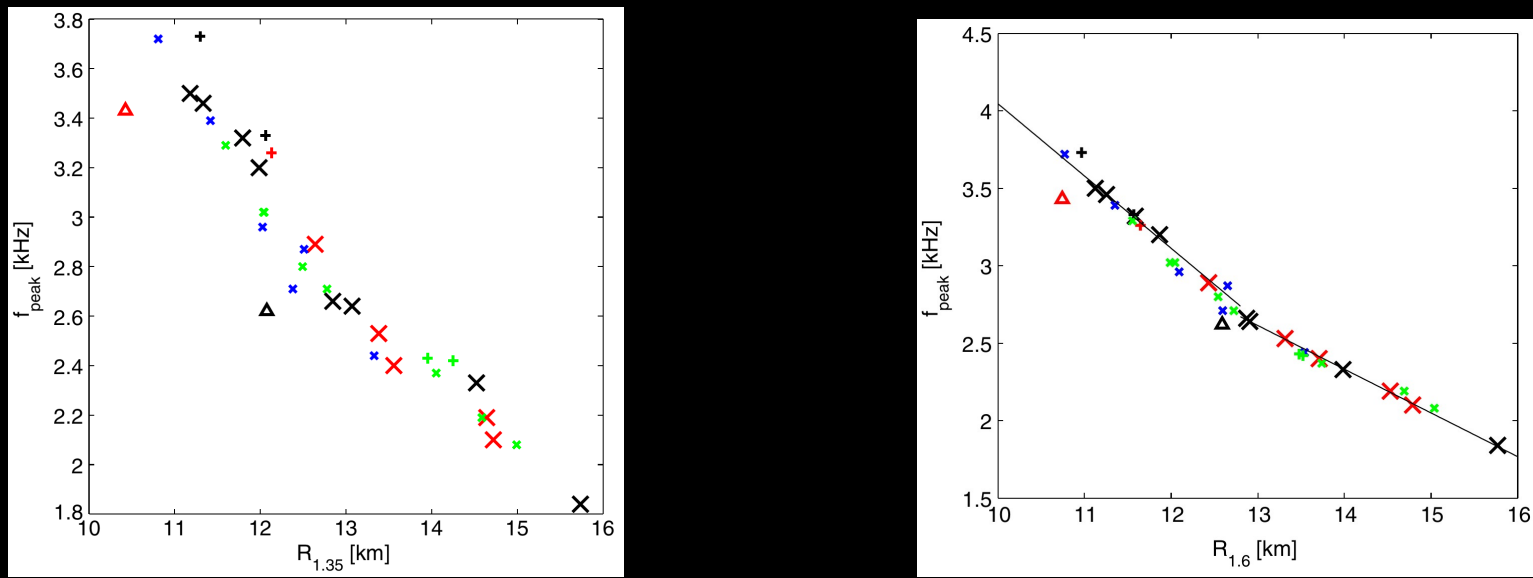
characterize EoS by radius of nonrotating NS with $1.35 M_{\text{sun}}$

Bauswein et al. 2012

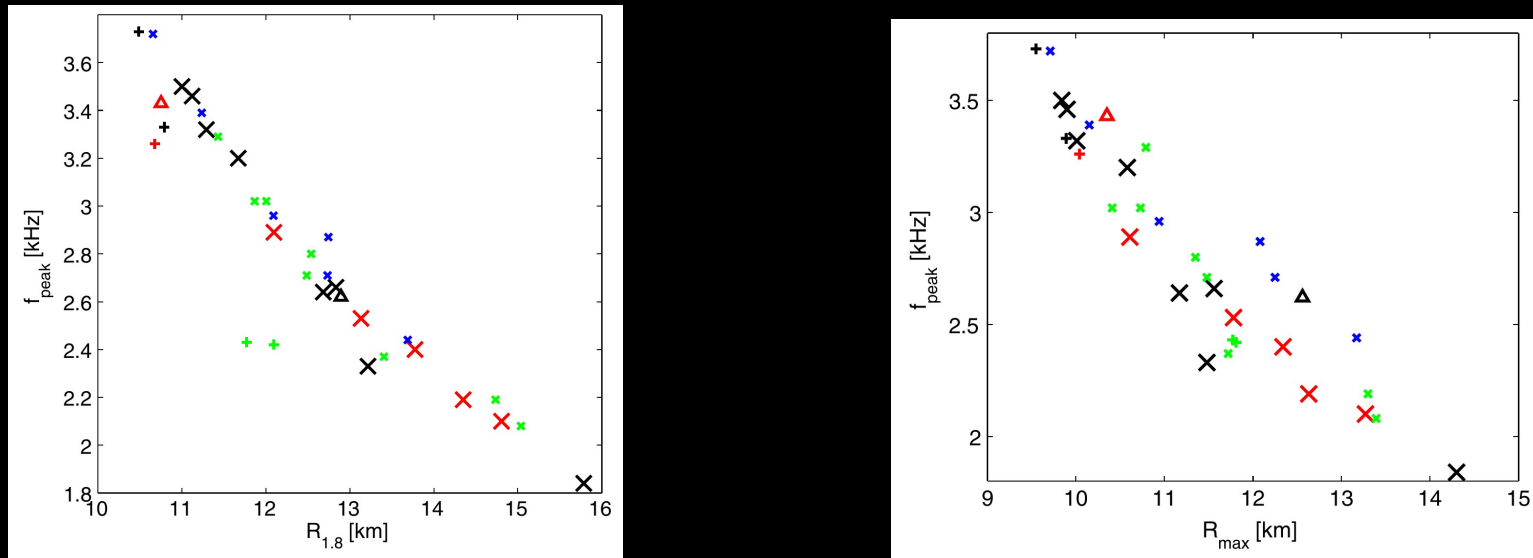
Pure TOV/EoS property => Radius measurement via f_{peak}

Here only 1.35-1.35 M_{sun} mergers (binary masses measurable) – similar relations exist for other fixed binary setups !!!

~ 40 different NS EoSs

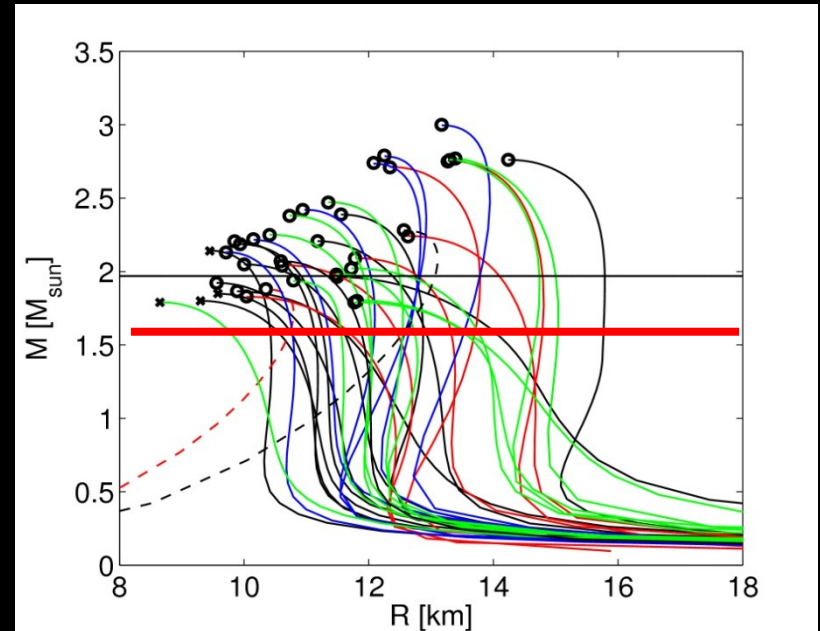
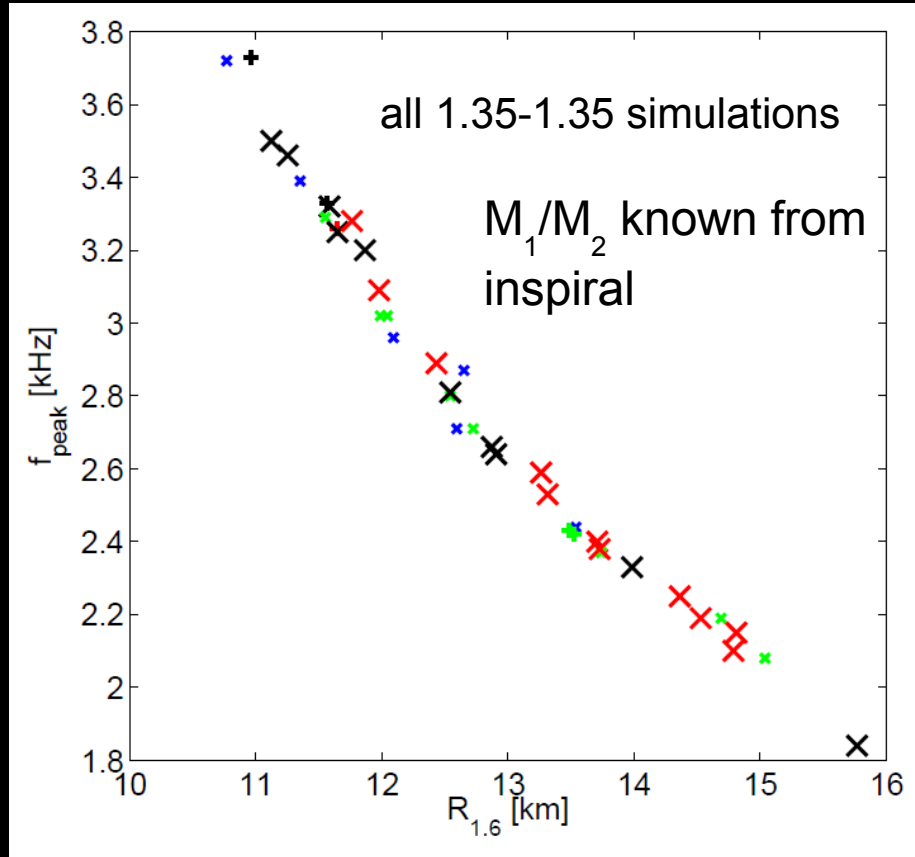


Bauswein et al. 2012



Assess quality of empirical relation – only infinity norm meaningful !!!
 → as many EoS models as possible !!!

Gravitational waves - EoS survey



characterize EoS by radius of nonrotating NS with $1.6 M_{\text{sun}}$

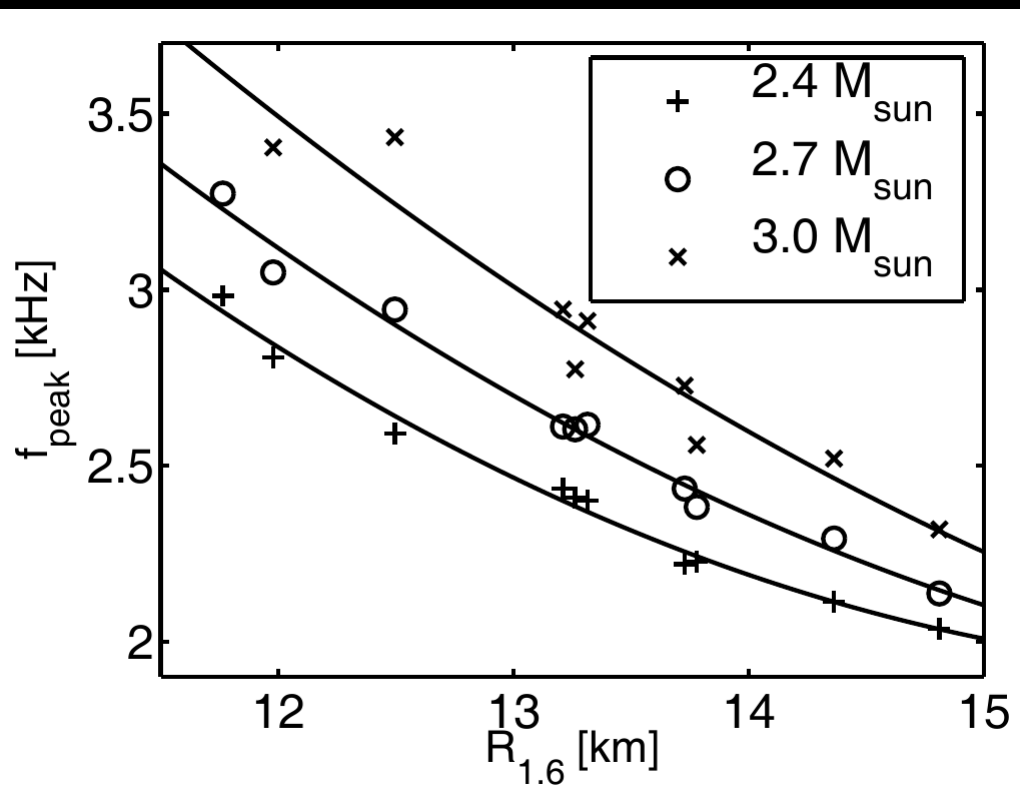
Bauswein et al. 2012

Pure TOV/EoS property => Radius measurement via f_{peak}

Smaller scatter in empirical relation (< 200 m) → smaller error in radius measurement

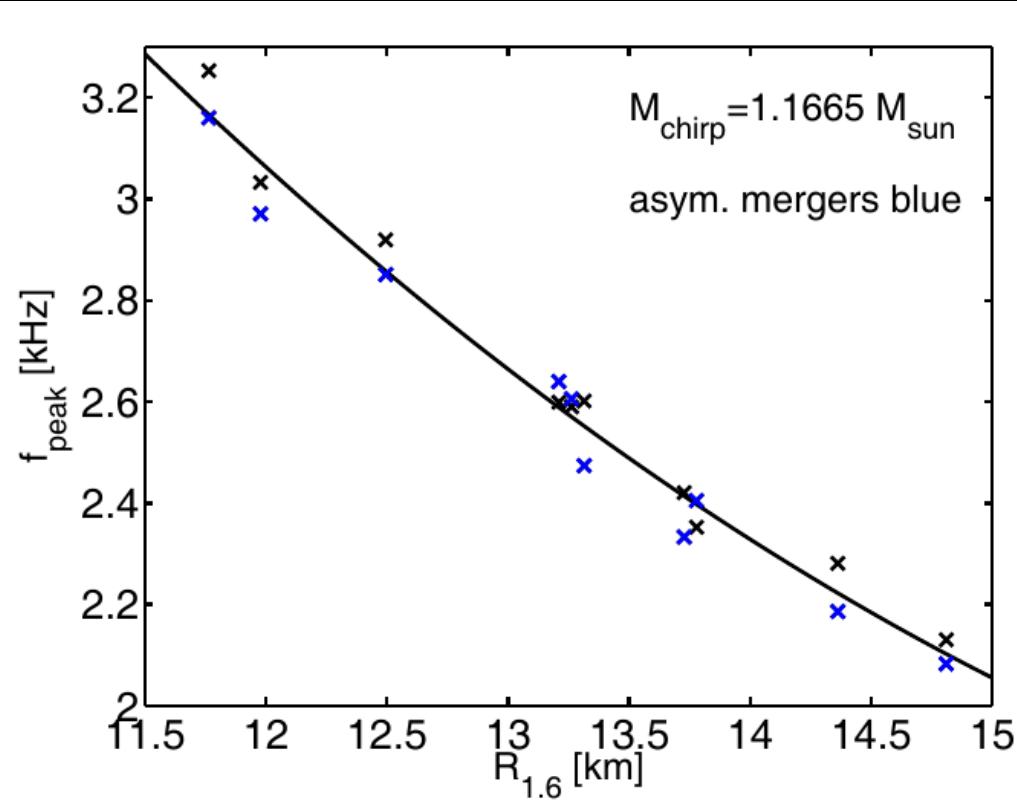
Note: R of $1.6 M_{\text{sun}}$ NS scales with f_{peak} from $1.35-1.35 M_{\text{sun}}$ mergers (density regimes comparable)

Binary mass variations



Different total binary masses
(symmetric)

Data analysis: see e.g. Clark et al. 2016 (PCA), Clark et al. 2014 (burst search), Chatzioannou et al 2017
→ f_{peak} precisely measurable !!!



Fixed chirp mass (asymmetric 1.2-1.5
 M_{sun} binaries and symmetric 1.34-
1.34 M_{sun} binaries)

Bauswein et al. 2012, 2016

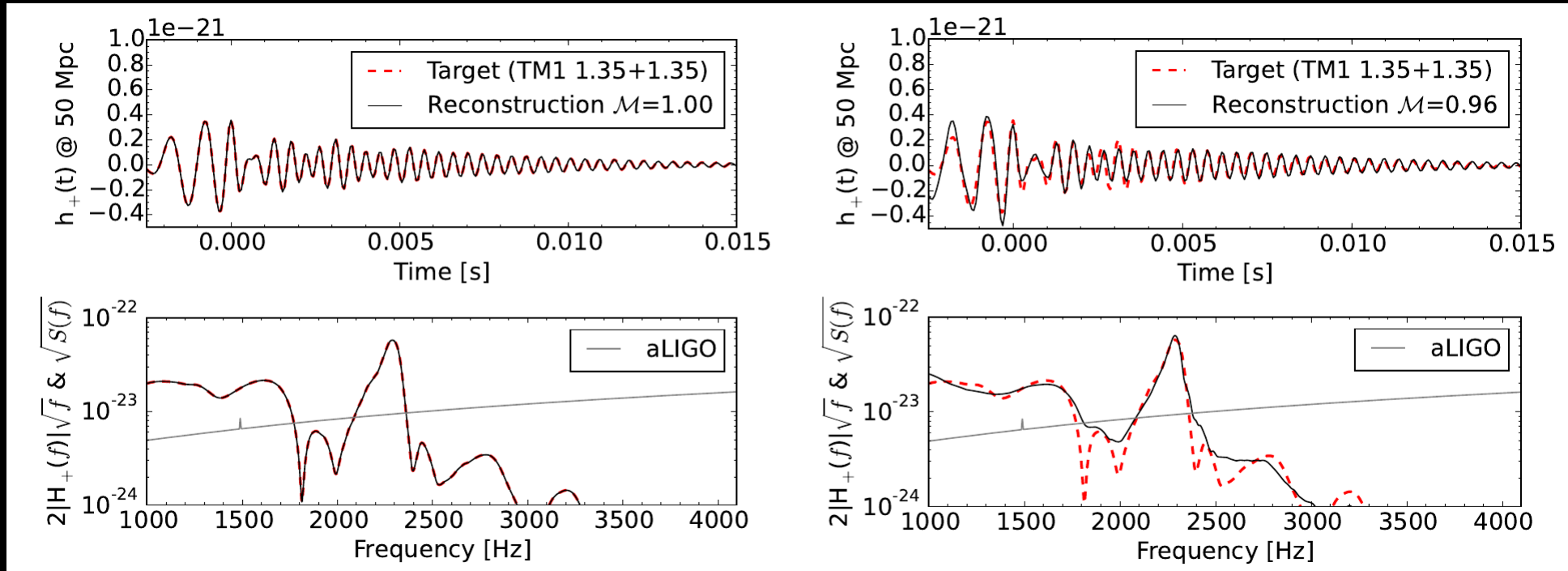
Strategy for radius measurements

- ▶ Measure binary masses from inspiral
- ▶ Construct $f_{\text{peak}} - R$ relation for this fixed binary masses and (optimally) chosen R
- ▶ Measure f_{peak} from postmerger GW signal
- ▶ Obtain radius by inverting $f_{\text{peak}} - R$ relation
- ▶ (possibly restrict to fixed mass ratios if mergers with high asymmetry are measured)

- ▶ Final error of radius measurement:
 - accuracy of f_{peak} measurement (see Clark et al. 2014, Clark et al. 2016)
 - maximum scatter in f-R relation (important to consider very large sample of EoSs)
 - systematic error in f-R relation

Data analysis

- Principal Component analysis



Excluding recovered waveform from catalogue

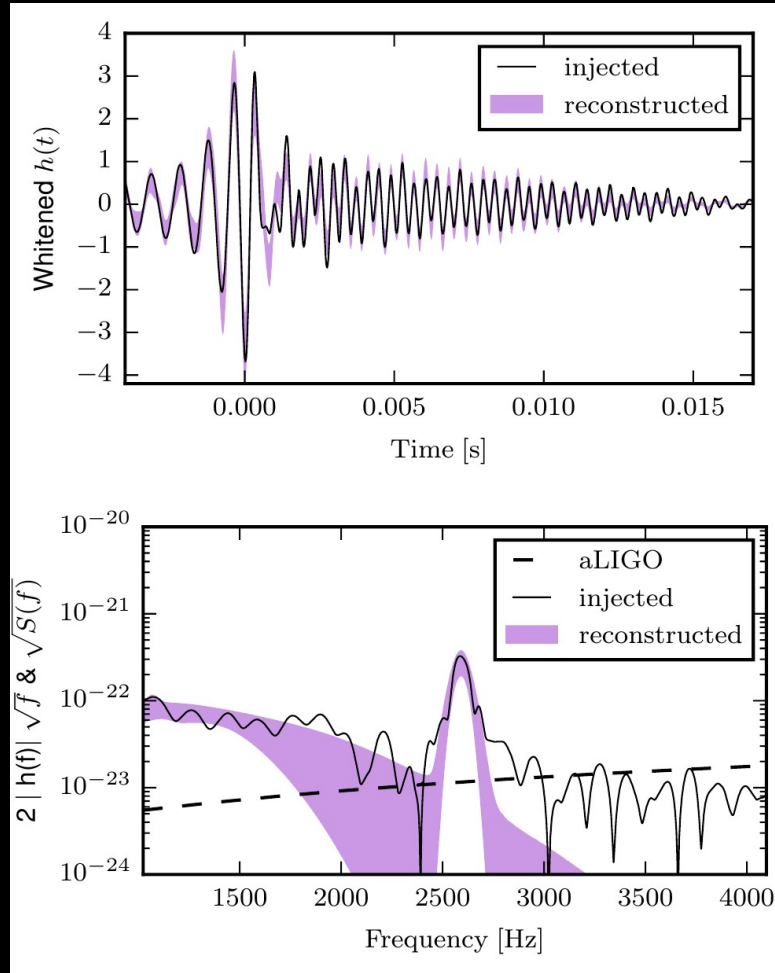
Clark et al. 2016, see also
 Clark et al 2014,
 Chatzioannou et al 2017,
 Bose et al. 2018

Instrument	SNR_{full}	D_{hor} [Mpc]	$\dot{\mathcal{N}}_{\text{det}}$ [year^{-1}]
aLIGO	$2.99^{3.86}_{2.37}$	$29.89^{38.57}_{23.76}$	$0.01^{0.03}_{0.01}$
A+	$7.89^{10.16}_{6.25}$	$78.89^{101.67}_{62.52}$	$0.13^{0.20}_{0.10}$
LV	$14.06^{18.13}_{11.16}$	$140.56^{181.29}_{111.60}$	$0.41^{0.88}_{0.21}$
ET-D	$26.65^{34.28}_{20.81}$	$266.52^{342.80}_{208.06}$	$2.81^{5.98}_{1.33}$
CE	$41.50^{53.52}_{32.99}$	$414.62^{535.221}_{329.88}$	$10.59^{22.78}_{5.33}$

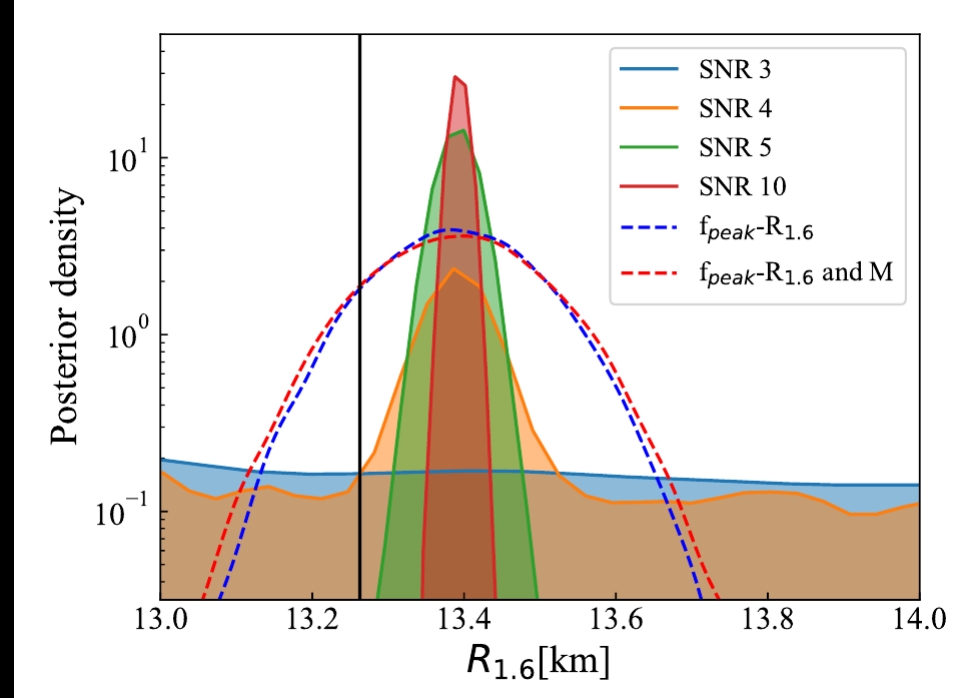
Outdated!!!

→ possible at Ad. LIGO's design sensitivity!

Model-agnostic data analysis



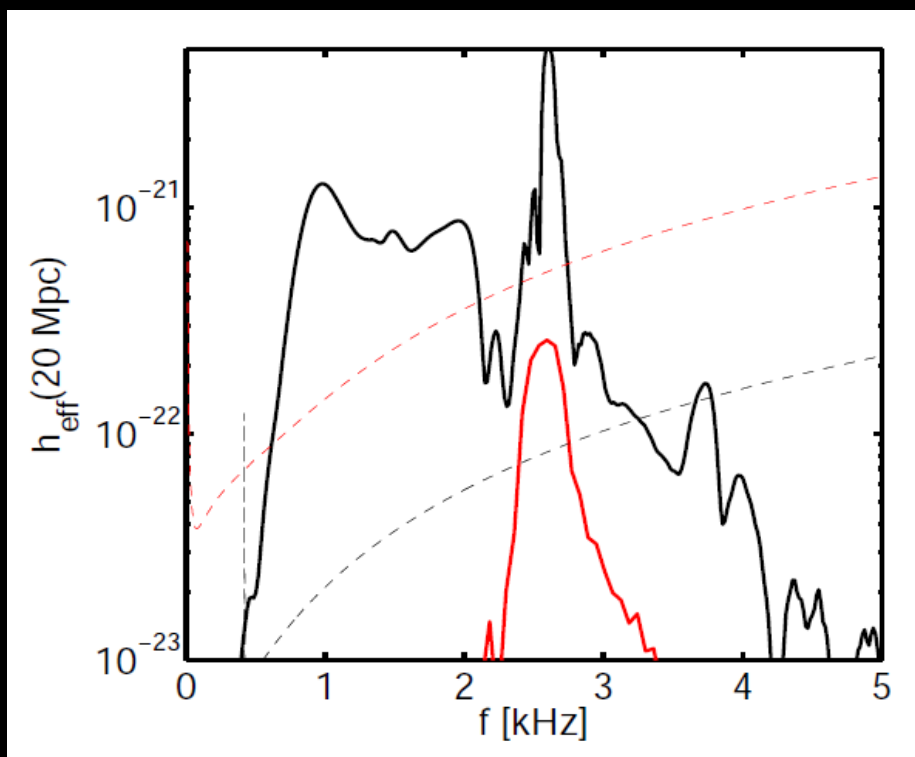
Based on wavelets



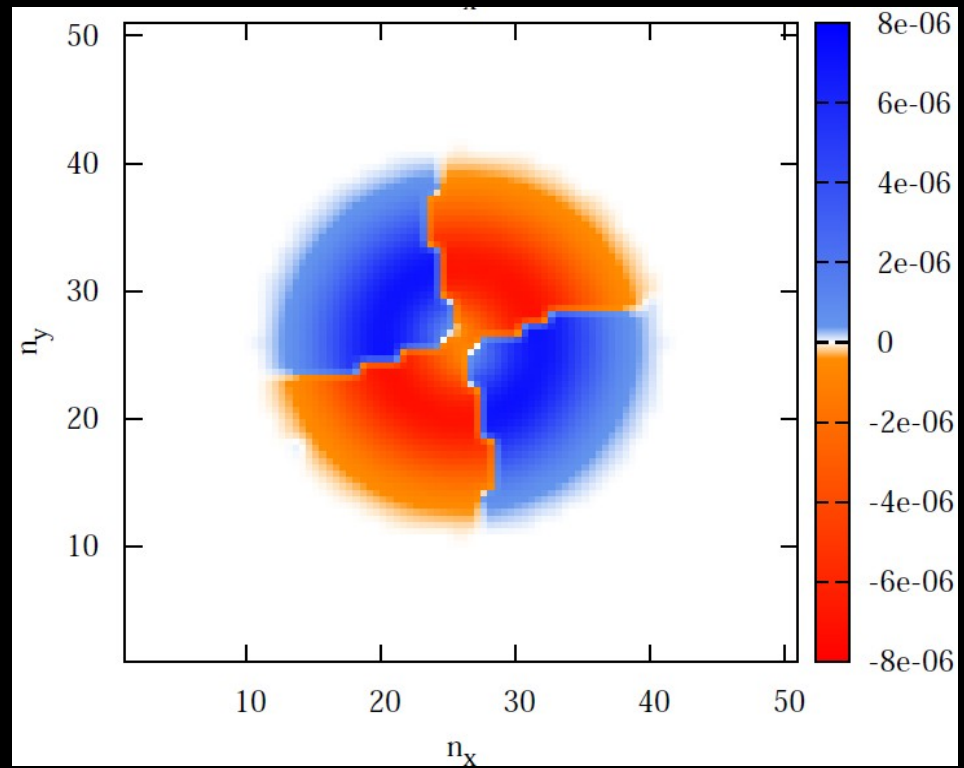
Chatzioannou et al. (2017)

Dominant oscillation frequency

- Fundamental quadrupolar fluid mode of the remnant



Re-excitation of f-mode ($|l|=|m|=2$)
in late-time remnant (Bauswein
et al. 2016)

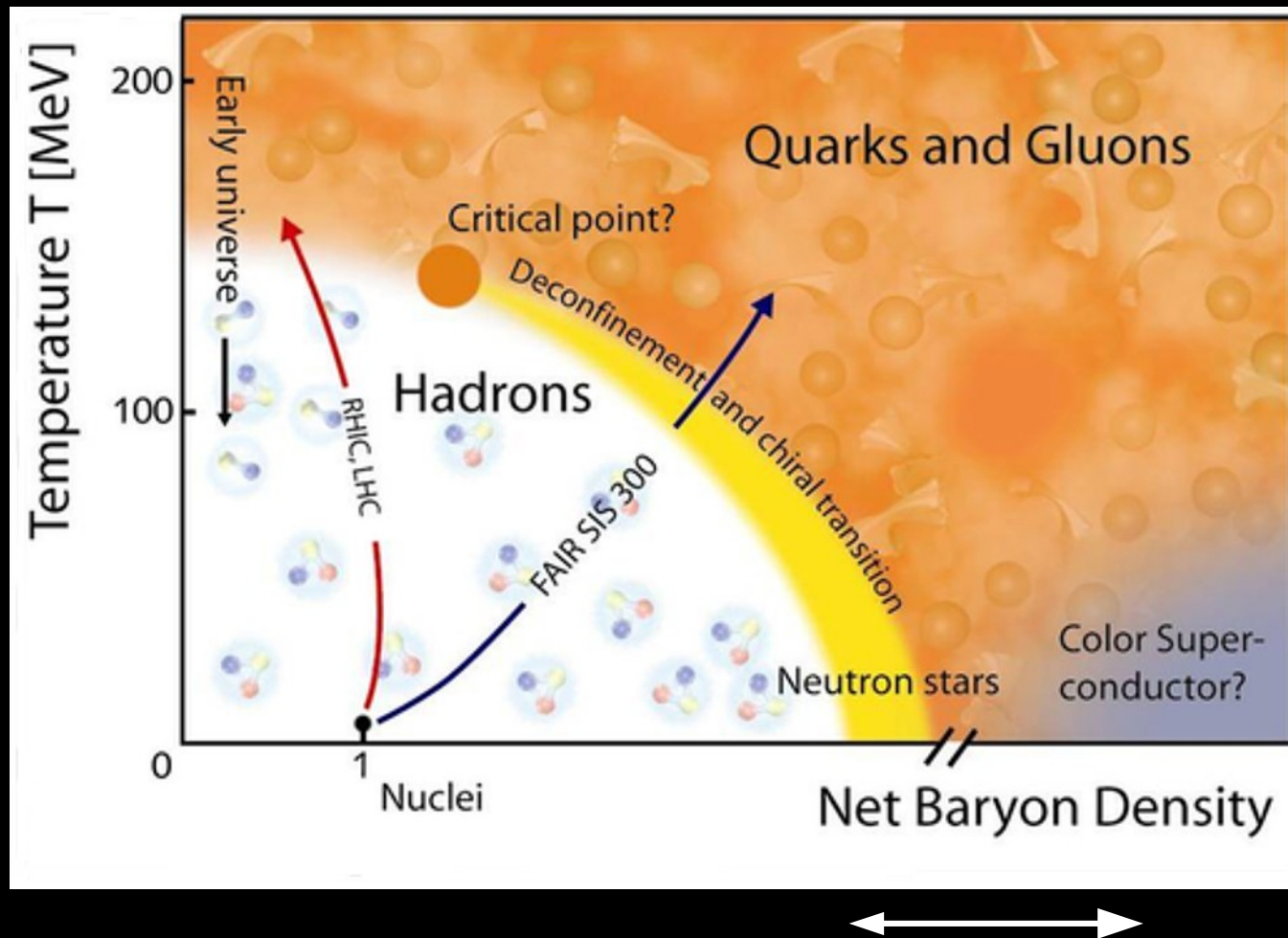


Mode analysis at $f=f_{\text{peak}}$
Stergioulas et al. 2011

Observable signature of (QCD) phase transition

Phase diagram of matter

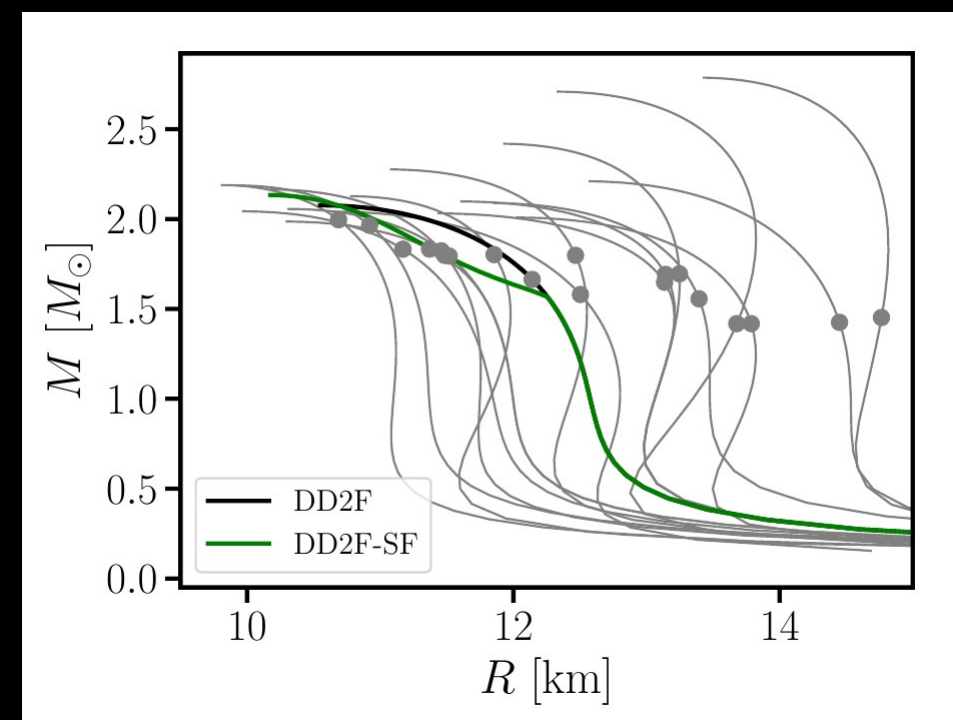
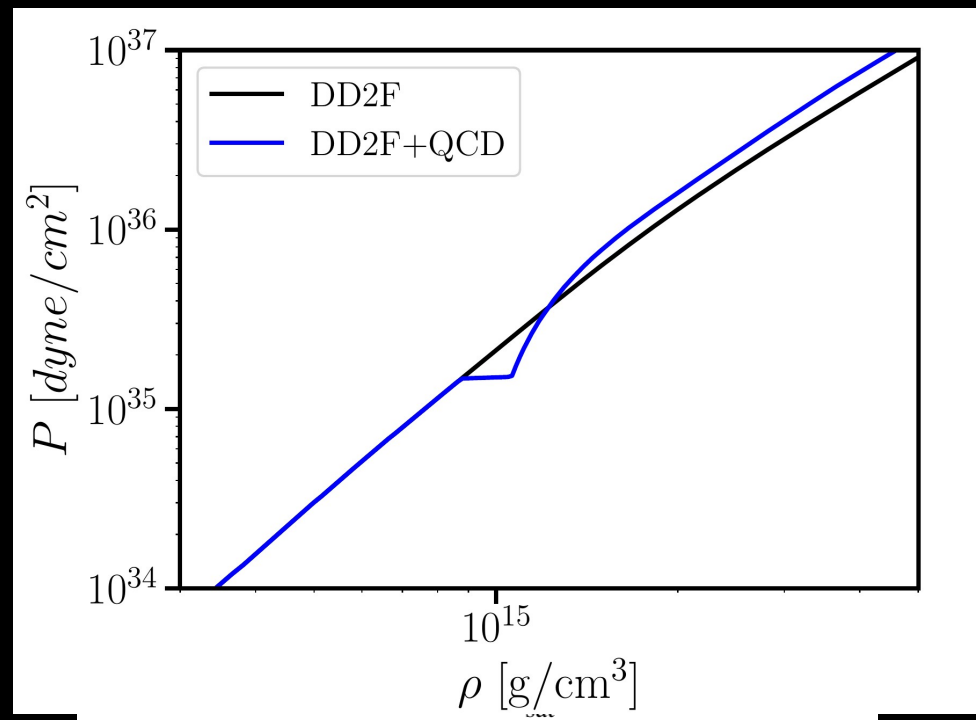
GSI/FAIR



Does the phase transition to quark-gluon plasma occur
(already) in neutron stars or only at higher densities?

EoS with 1st-order phase transition to quark matter

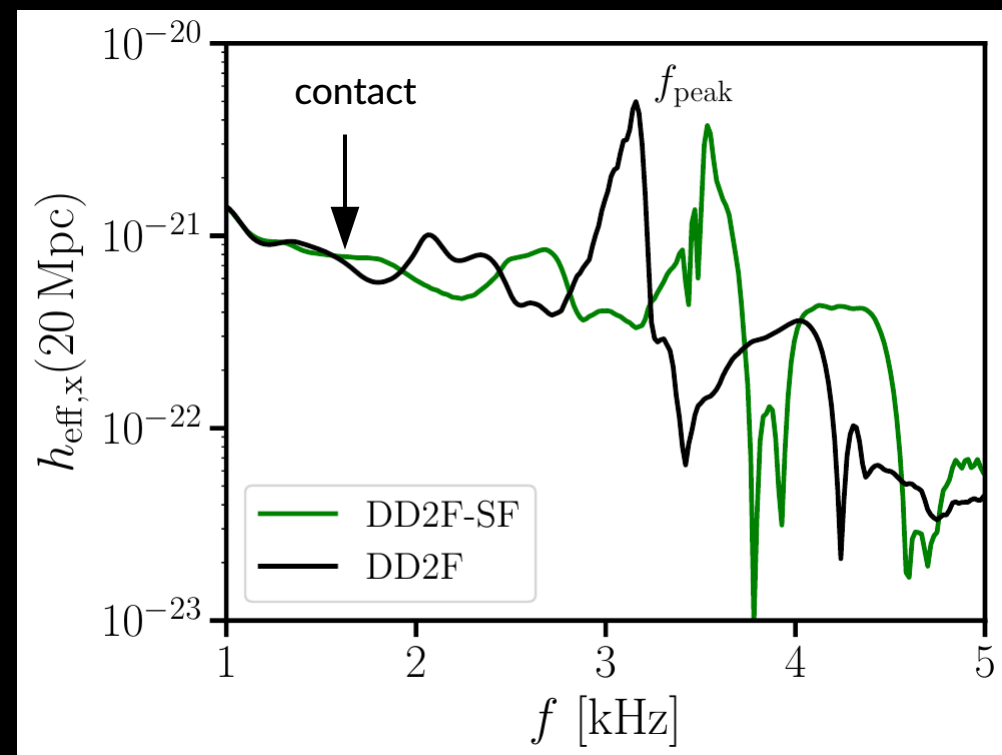
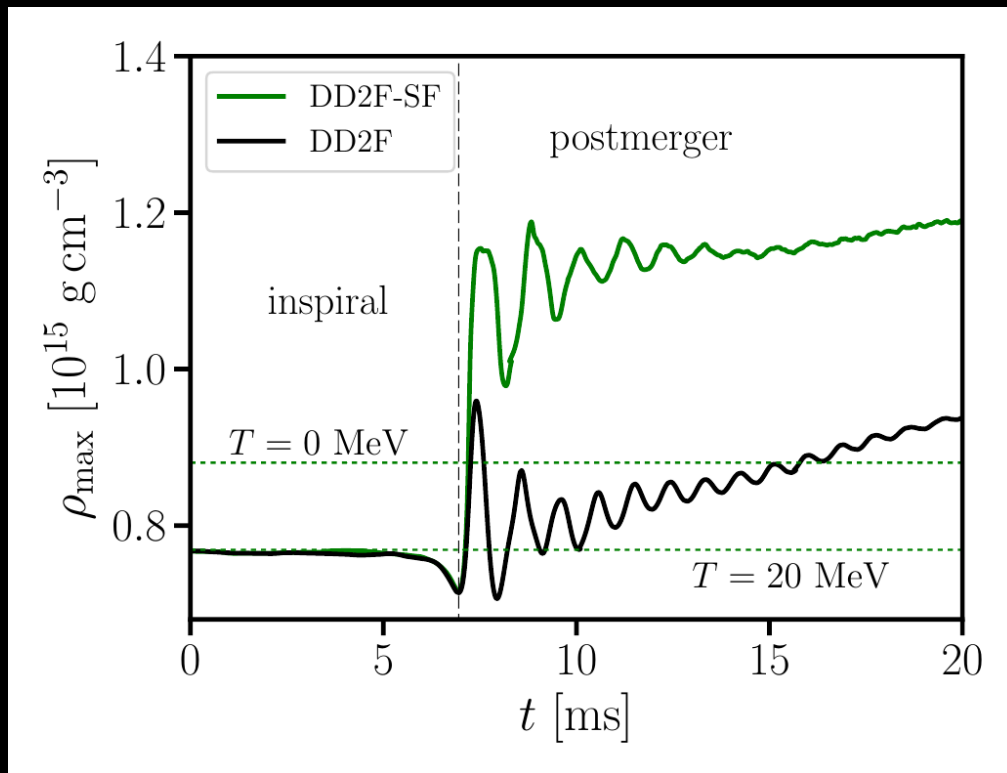
Bauswein et al. 2018



- EoS from Fischer et al. 2018 – as one example for an EoS with a strong 1st-order phase transition to deconfined quarks

Merger simulations

► GW spectrum 1.35-1.35 Msun

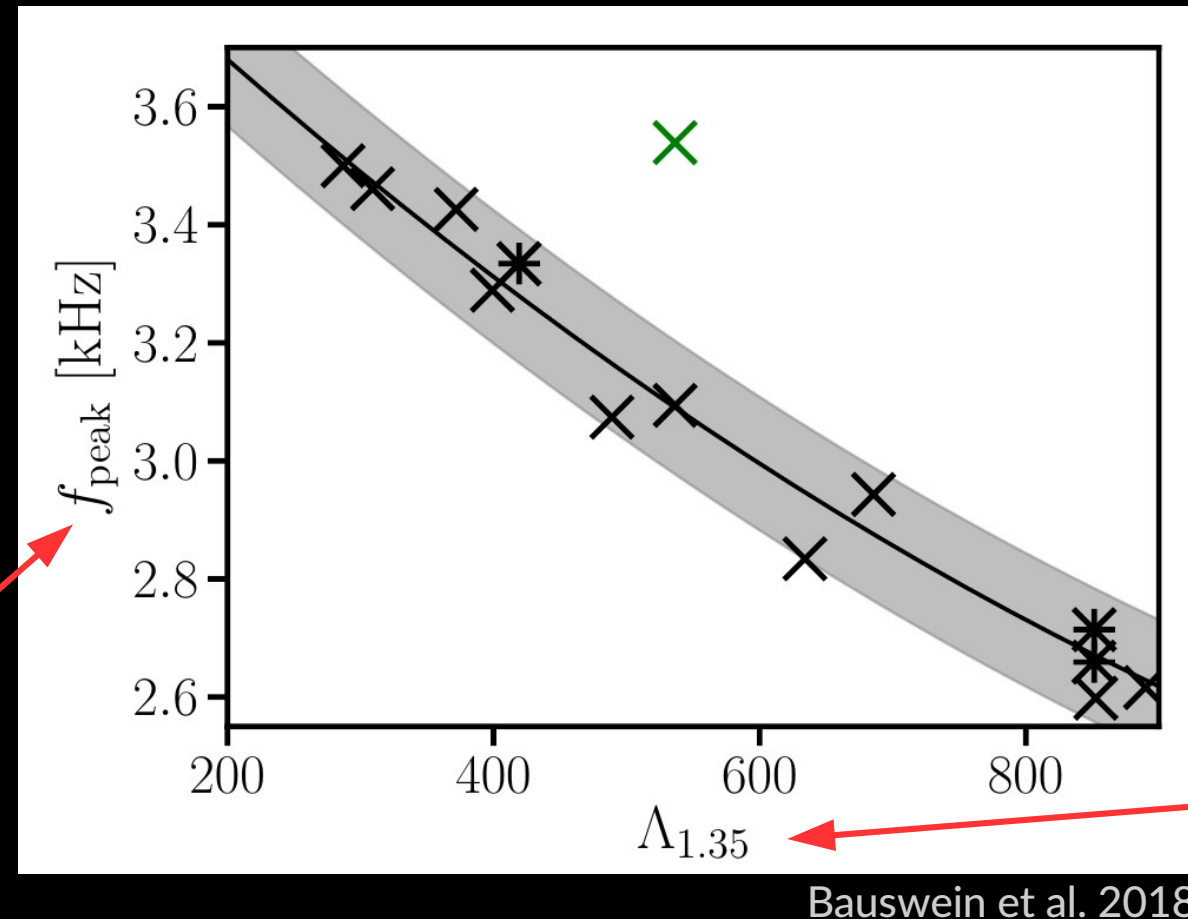


Bauswein et al. 2018

But: a high frequency on its own may not yet be characteristic for a phase transition
→ unambiguous signature
(→ show that all purely baryonic EoS behave differently)

Signature of 1st order phase transition

from postmerger

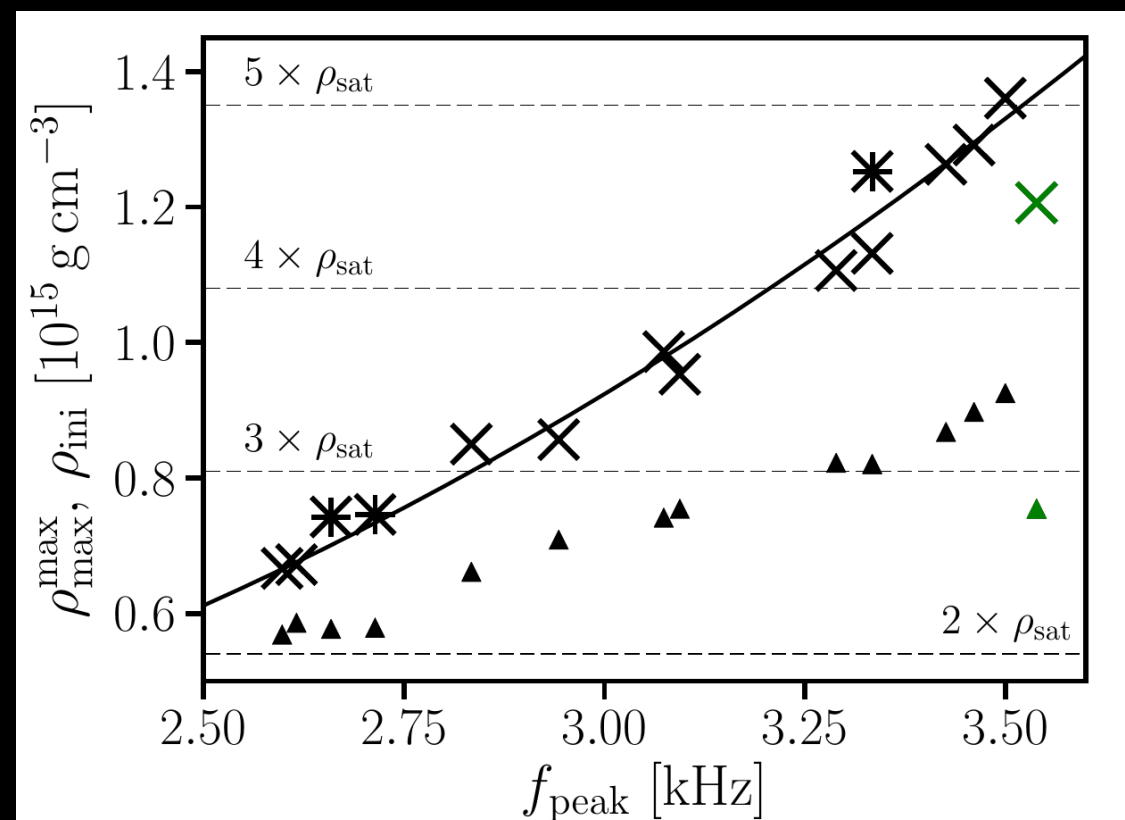


- ▶ Tidal deformability measurable from inspiral to within 100-200 (Adv. Ligo design)
- ▶ Postmerger frequency measurable to within a few 10 Hz @ a few 10 Mpc (either Adv. Ligo or upgrade)
- ▶ Important: “all” purely hadronic EoSs (including hyperonic EoS) follow f_{peak} -Lambda relation → deviation characteristic for strong 1st order phase transition

Discussion

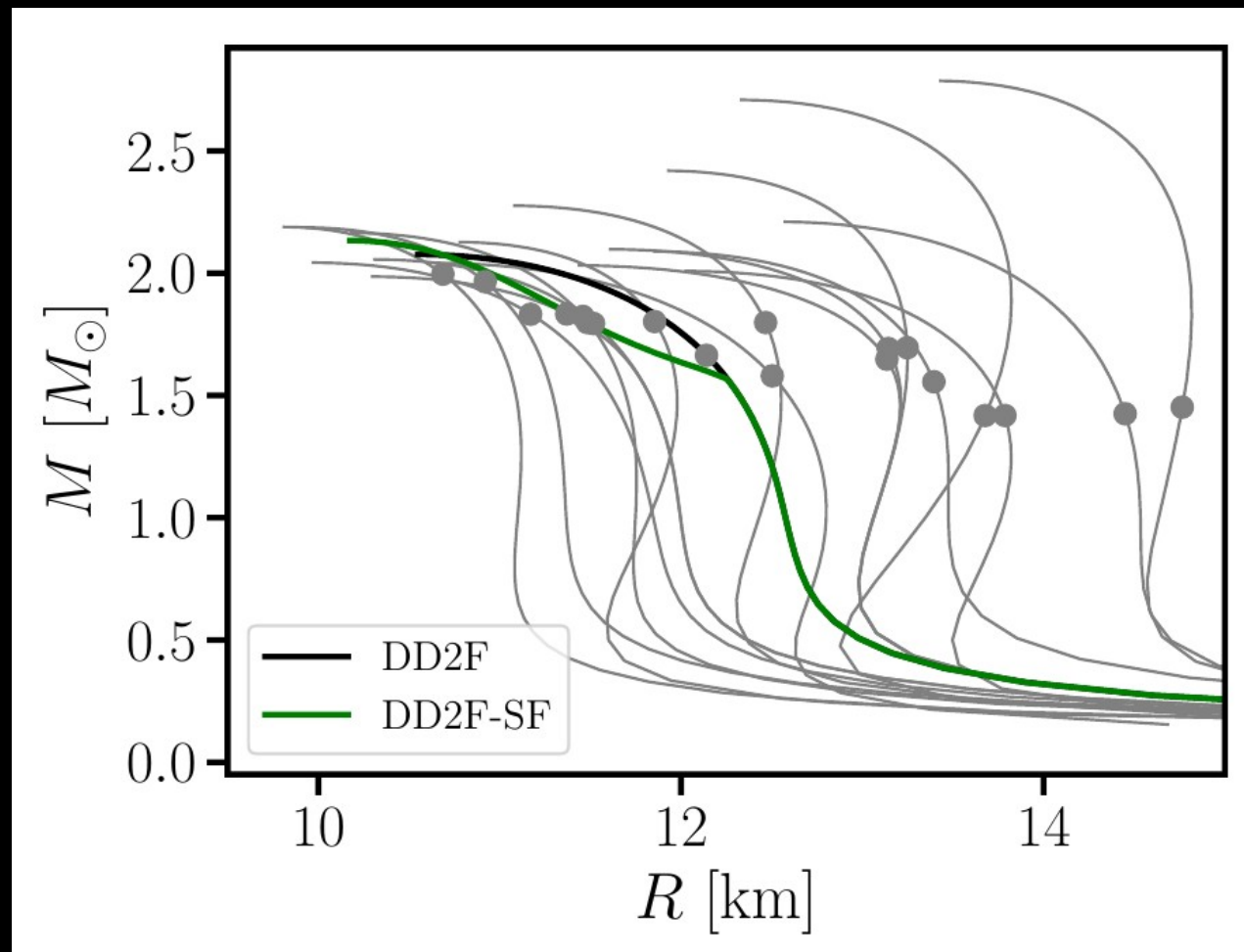
- ▶ Consistency with fpeak-Lambda relation points to
 - purely baryonic EoS
 - (or at most weak phase transition → no strong compactification)in the tested (!) density regime
- ▶ fpeak also determines maximum density in postmerger remnant
- ▶ postmerger GW emission provides complimentary information to inspiral
→ probes higher density regime

Bauswein et al. 2018



Probed densities / NS masses

- Dots: NS mass with central density = maximum density during early postmerger evolution



For 1.35-1.35 Msun merger – higher binary masses probe higher densities / NS masses

Conclusions

- ▶ Ejecta properties inferred from GW170817 compatible with simulation results
- ▶ Tidal deformability = EoS property affecting phase evolution during late inspiral
- ▶ Tidal deformability constrained from above → rules out stiff nuclear matter / large NS radii
- ▶ Multi-messenger interpretation based on minimal assumptions: NS radius must be larger than 10.7 km (very robust)
- ▶ More stringent constraints from future detections
- ▶ NS radius measurable from dominant postmerger frequency
- ▶ Explicitly shown by GW data analysis
- ▶ Threshold binary mass for prompt collapse → maximum mass M_{\max}
- ▶ Strong 1st order phase transitions leave characteristic imprint on GW (postmerger frequency higher than expected from inspiral)
- ▶ Complementarity of inspiral and postmerger phase → postmerger probes higher density regime